# Simulation of fixed bed adsorption processes with simplified models. Application for $CO_2$ adsorption in biogas purification.

**María Eugenia Inchauspe**

Final dissertation submitted to **Escola Superior de Tecnologia e Gestão** of **Instituto Politécnico de Bragança** to obtain the Master Degree in **Chemical Engineering** in the ambit of the double diploma with the **Universidad Tecnológica Nacional – Facultad Regional Córdoba**

Supervisors

**Prof. Doctor João Paulo Almeida**

**Prof. Doctor José António Silva**

**Prof. Doctor María Soledad Renzini**

Bragança

2020

*Things work out best for those who make*

*the best of how things work out.*

*John Wooden*

**ACKNOWLEDGEMENTS**

I would like to thank all the people who have contributed to make this thesis possible. First of all to my tutors Prof. Doctor João Paulo Almeida and Prof. Doctor José António Silva, for their support and guidance throughout the process.

To the Instituto Politécnico de Bragança, for receiving me and giving me the opportunity to carry out this double diploma program. To the Universidad Tecnológica Nacional-Facultad Regional Córdoba for having been the institution in wich I first trained as a professional and for giving me the opportunity to carry out this program.

A special thanks to my co-tutor Prof. Doctor Soledad Renzini, for her patience, for the learnings that I achieved thanks to her and for her commitment to my process.

To my colleagues with whom I shared the double degree program, who were my family in this time away from home. Finally to my family who are always a support in each of my achievements.

**ABSTRACT**

Biogas production has grown remarkably in recent years and this growth is expected to continue in the coming years. This growth leads to an increase in the field of biogas purification and upgrading research. Among the variety of existing purification and upgrading techniques, one of the most used today is adsorption, specifically Pressure Swing Adsorption (PSA) as it is convenient when a cost-efficiency balance is made. To describe the dynamic behavior of an adsorption column, it is necessary to know the effluent concentration-time profile, also called the breakthrough curve. A good prediction of the breakthrough curve is essential to ensure the normal and safe operation of the process. Among the existing mathematical models to make this prediction, the Bohart-Adams model is one of the oldest and simplest in terms of mathematical application. This model considers that the operation is carried out at a constant velocity, but when the feed concentration is high, as in the case of biogas purification where we can have $CO_2$ concentrations of up to 50%, the velocity cannot be considered constant. In this work, the different forms of the Bohart-Adams equation were studied and it was observed that this model, Tomas's and Yoon Nelson's are the same with minor modifications. The main advantage of the use of a mathematically simple model such as Bohart-Adams for the design and scale-up in an adsorption process is to shorten the times in determining the design variables and construction parameters of the equipment and this advantage is accompanied by a reduction in costs in the design and calculation stage of the process. Seeking to transfer the mathematical simplicity of this equation to cases in which high concentrations are used, tests were performed using the Bohart-Adams logistic form, studying the changes in the fit of the experimental data when a correction for variable velocity is applied in the stoichiometric time calculation. These tests were carried out with three types of adsorbents along with three different concentrations, the three adsorbents were: Activated Carbon, Pellets CuBTC and Bulk CuBTC and the concentrations used were 20%, 33% and 50% $CO_2$. It was found that using the sigmoid or logistic form of Bohart-Adams, good adjustments were achieved even with initial concentrations of 50%. In the end, it is shown how the parameters obtained from this model are useful to make a scale-up in a simple way.

**RESUMO**

A produção de biogás cresceu notavelmente nos últimos anos e espera-se que esse crescimento continue nos próximos anos. Este crescimento leva a um aumento no campo da purificação do biogás e pesquisa de atualização. Entre a variedade de técnicas de purificação e atualização existentes, uma das mais usadas hoje é a adsorção, especificamente a Adsorção por Variação de Pressão (PSA), pois é conveniente quando é feito um equilíbrio de custo-benefício. Para descrever o comportamento dinâmico de uma coluna de adsorção, é necessário conhecer o perfil concentração-tempo do efluente, também chamado de curva de ruptura. Uma boa previsão da curva de ruptura é essencial para garantir o funcionamento normal e seguro do processo. Dentre os modelos matemáticos existentes para fazer essa previsão, o modelo Bohart-Adams é um dos mais antigos e simples em termos de aplicação matemática. Este modelo considera que a operação é realizada a uma velocidade constante, mas quando a concentração de alimentação é alta, como no caso da purificação do biogás onde podemos ter concentrações de $CO_2$ de até 50%, a velocidade não pode ser considerada constante. Neste trabalho, as diferentes formas da equação de Bohart-Adams foram estudadas e observou-se que este modelo, o de Tomas e o de Yoon Nelson são iguais, com pequenas modificações. A principal vantagem do uso de um modelo matematicamente simples como Bohart-Adams para o projeto e aumento de escala em um processo de adsorção é encurtar os tempos na determinação das variáveis de projeto e parâmetros de construção do equipamento e esta vantagem é acompanhada por um redução de custos na fase de desenho e cálculo do processo. Em busca de transferir a simplicidade matemática desta equação para os casos em que são utilizadas altas concentrações, foram realizados testes utilizando a forma logística de Bohart-Adams, estudando as alterações no ajuste dos dados experimentais quando uma correção para velocidade variável é aplicada no estequiométrico cálculo do tempo. Estes testes foram realizados com três tipos de adsorventes juntamente com três concentrações diferentes, os três adsorventes foram: Carvão Ativado, Pellets CuBTC e Bulk CuBTC e as concentrações utilizadas foram 20%, 33% e 50% $CO_2$. Verificou-se que usando a forma sigmóide ou logística de Bohart-Adams, bons ajustes foram alcançados mesmo com concentrações iniciais de 50%. Ao final, mostra-se como os parâmetros obtidos neste modelo são úteis para fazer um scale-up de forma simples.

# LIST OF CONTENTS

*Chapter 1* - INTRODUCTION ..... 1

1.1 Motivations and objectives ..... 2

1.2 State of the art ..... 5

*1.2.1* Biogas Production ..... 5

*1.2.2* Biogas upgrading and purification ..... 9

*1.2.3* *Upgrading technologies* ..... 11

*1.2.4* Advantages and disadvantages of biogas upgrading technologies ..... 18

*1.2.5* *Pressure swing adsorption (PSA)* ..... 20

*1.2.6* Adsorbents for PSA technology ..... 21

*1.2.7* Simple mathematical models for the Adsorption Process ..... 28

*Chapter 2* – MATHEMATICAL MODELING AND SIMULATION ..... 29

2.1 Introduction ..... 30

2.2 Mathematical modeling and simulation ..... 30

2.3 Mathematical modeling and simulation in adsorption ..... 31

2.4 The Bohart-Adams model ..... 34

*2.4.1* Validity of the Bohart-Adams model ..... 36

*2.4.2* Parameter estimation of the Bohart-Adams model ..... 39

2.5 Mathematical modeling and scale-up applied to biogas purification and upgrading ..... 41

*Chapter 3* – METHODOLOGY AND EXPERIMENTAL STUDY ..... 43

3.1 Introduction ..... 44

3.2 Methodology ..... 44

3.3 Experimental study ..... 44

*3.3.1* Bulk activated carbon, AC ..... 45

*3.3.2* Crystalline powder, bulk CuBTC ..... 46

*3.3.3* Crystalline pellets, pelleted CuBTC ..... 49

3.4 Scaling-up from the Bohart-Adams model ..... 50

*Chapter 4* – CONCLUSIONS AND FUTURE PERSPECTIVES ..... 53

4.1 Conclusions ..... 54

4.2 Future perspectives ..... 55

BIBLIOGRAPHIC REFERENCE ..... 56

# *Chapter 1* - INTRODUCTION

## 1.1 Motivations and objectives

Biogas is a precious source of renewable energy, that could be the substitute for natural gas and fossil fuels, its use and production has been increasing for some years now. It is produced by degradation of organic matter under anaerobic conditions, this process is called Anaerobic Digestion. Biogas is mainly composed of methane and carbon dioxide in ranges of 50-70% and 30-50% respectively. It can also contain in lower concentrations other gases such as: nitrogen at concentrations of 0–3%, vapour water at concentrations of 5-10%, oxygen at concentrations of 0–1%, hydrogen sulfide at concentrations of 0–10,000 ppmv, ammonia at concentrations of 0–200 mg $m^{-3}$, benzene 0.6-35.6 mg $m^{-3}$, toluene 1.7-7 mg $m^{-3}$ and siloxanes at concentrations of 0–41 mg $m^{-3}$ [1]. The upgrading, purification and uses of biogas as a substitute for natural gas has gained importance in recent years and has been and is being widely discussed, due to the increase in energy demand and the need to change energy production processes towards more friendly systems, environmentally talking [2,3].

Same environmental advantages of biogas utilization are:

1. It is used as a renewable energy source.
2. It reduces the $CH_4$ emission to the environment.
3. It can be used as a substitute for fossil fuels.
4. It reduces the emission of $CO_2$ from combustion.
5. It can be used in all natural gas appliances after upgrading.

According to the Annual report 2019 of European Biogas Association (EBA), which collects data until 2018, the number of biogas plants has increased considerably in Europe in recent years, while in 2009 there were 6,227 biogas plants, in 2018 it reached 18,202. This growth is expected to continue as Europe aims by 2050 to thrive on a fully renewable energy system [4].

The mainly applications of biogas are:

1. $H_2$ production.
2. Electricity and power generation with combined heat and power production (CHP).
3. Injection into the natural gas grids after upgrading.
4. Production of heat and steam.
5. As a vehicular fuel in upgraded and compressed form.

Each of these applications requires specific biogas compositions, *Table 1*, and this is why, with the growth in the production and use of biogas, there have been advances in studies of different methods of upgrading and purification.

*Table 1. Biogas types and its composition.*

| | Landfills | Sewage digesters | Agricultural waste | Livestock waste | Organic waste digesters |
|---|---|---|---|---|---|
| $CH_4$ (%) | 45-60 | 58-65 | 50-80 | 50-80 | 60-70 |
| $CO_2$ (%) | 24-40 | 33-40 | 30-50 | 30-50 | 30-40 |
| $N_2$ (%) | 1-17 | 1-8 | 0-1 | 0-1 | 1 |
| $O_2$ (%) | 1-26 | <1 | 0-1 | 0-1 | 1-5 |
| $H_2S$ (%) | 15-427 | 0-24 | 0.01-0.07 | 0-1 | 10-180 |
| Benzene (mg $m^{-3}$) | 0.6-35.6 | 0.1-0.3 | traces | traces | 0.1-1.1 |
| Toluene (mg $m^{-3}$) | 1.7-287 | 2.8-11.8 | traces | traces | 3-7 |
| Ref. | [5-7] | [5,8,9] | [10] | [10] | [5] |

KHAN, et al. [2] compared different technologies of upgrading and purification and they showed that adsorption still continues to be one of the most efficient and economically convenient options.

The adsorption process can be carried out in a closed system that contains a certain amount of adsorbent in contact with a certain volume of adsorbate solution, this is called Batch-adsorption. Or it may occur in an open system where the adsorbate solution is continuously passed through a column packed with adsorbent, this is called Fixed-bed-adsorption [11]. In this work we focus our attention on the latter, since it is the one with the greatest industrial application.

To determine the dynamic behavior of a fixed-bed column, we must know the effluent concentration profile, the breakthough curve. This curve is determined from the equilibrium isotherm data and by the individual transport processes within the column [12]. For the design of a fixed-bed adsorption column it is necessary to be able to predict the breakthrought curve. In this sense, mathematical models have a fundamental role to understand the dynamic of these columns, as well as for the design and optimization of these processes [13]. The determination of the breakthrough curve is a issue of great importance since it contains the basic information for a good design of an adsorption column. Without this information, it is impossible to determine a scaling of an adsorption column for practical application. The breakthrough curve could be obtained in two ways: the first one direct experimentation with this is obtained concise information of the breakthrough, but it generally takes a long time and is an economically undesired process, especially in the case of components with high residence times. Also, it depends on experimental conditions such as temperature. The second way is mathematical modeling, it is simple and realizable with not

experimental apparatus required. For this reason, mathematical modeling has attracted increasing interest in recent decades. The general way to predict the breakthrough curve by mathematical modeling, is to solve a set of partial differential equations which consist of a macroscopic mass conservation equation, uptake rate equation (sometimes including a set of equations), and isotherm equation, together with a set of initial and boundary conditions. Proposing a general use model is an important but challenging task, taking into account the particularities of each system (solvents, adsorbate, adsorbent), the variable operating conditions and the specific demands of precision and calculative simplicity, and also considering that many models derived from different assumptions are valid for limited situations and fail to describe others systems [11].

Among the various existing models to determine the breakthrough curve, the Bohart–Adams model has been used in many sorption process modeling studies, due it is mathematical simplicity [11]. When the component to be adsorbed is at low concentrations, the gas velocity in the adsorption column can be considered constant and the Bohart-Adams model was originally developed under this assumption. Yet, in the adsorption of $CO_2$ in biogas, typically we speak of concentrations that can reach up to 50% and the speed of adsorption has influence in the process. Therefore, in these cases the speed cannot be consider constant anymore and this has implications on the Bohart-Adams model. In other words, the mathematical simplicity of Bohart-Adams model derives from considering the velocity of adsorption as constant. When dealing with high concentration levels of adsorbed species (nontrace systems), as is the case of $CO_2$ adsorption in biogas, the model does not behave well and the predicted breakthrough curve is out of step with the real curve, observed by the empirical values.

Among the advantages of using a mathematically simple model such as the Bohart-Adams one is the potential to simplify the scaling process, which sometimes needs to be done in several stages, to bring adsorption from a laboratory scale to an industrial scale. This simple math allows the process to be less time-consuming and therefore more economical. Therefore the goal of this work is to analyses different forms of the Bohart-Adams model in order to make it suitable for correct prediction of the breakthrough curve also in the case of high concentration of adsorbed species and also show how, starting from a simple modeling carried out with Bohart-Adams through a series of simple steps, the scale-up can be obtained on an large scale process.

## 1.2 State of the art

### *1.2.1* Biogas Production

Anaerobic digestion is a biochemical process in which complex organic matter is decomposed by microbial action in the absence of oxygen. This process is common in many natural environments such as marine water sediments. Industrially it is used for the production of biogas. In many of these facilities it is common to use a homogeneous mixture of two or more feedstock types, for example animal sludge and organic waste from food industries, in these cases the process is called co-digestion.

For the production of biogas, a wide variety of biomass types can be used as substrate (feedstock). The most common are: animal manure and slurry, agricultural residues and by-products, digestible organic wastes from food and agro industries (vegetable and animal origin), organic fraction of municipal waste and from catering (vegetable and animal origin), sewage sludge, dedicated energy crops (e.g. maize, miscanthus, sorghum, clover).

***Anaerobic digestion***

As indicated previously, the production of biogas is carried out by a microbiological process of decomposition of organic matter in the absence of oxygen. As a co-product, the digestate is obtained and it is the decomposed substrate. During this process a series of linked steps occur with a very little heat is generated. In these stages the material continually breaks down into smaller units. In each step, specific groups of microorganisms successively decompose the products of the previous steps. *Figure 1* is a simplified representation of this anaerobic digestion process. The main process steps are: hydrolysis, acidogenesis, acetogenesis and methanogenesis [14].

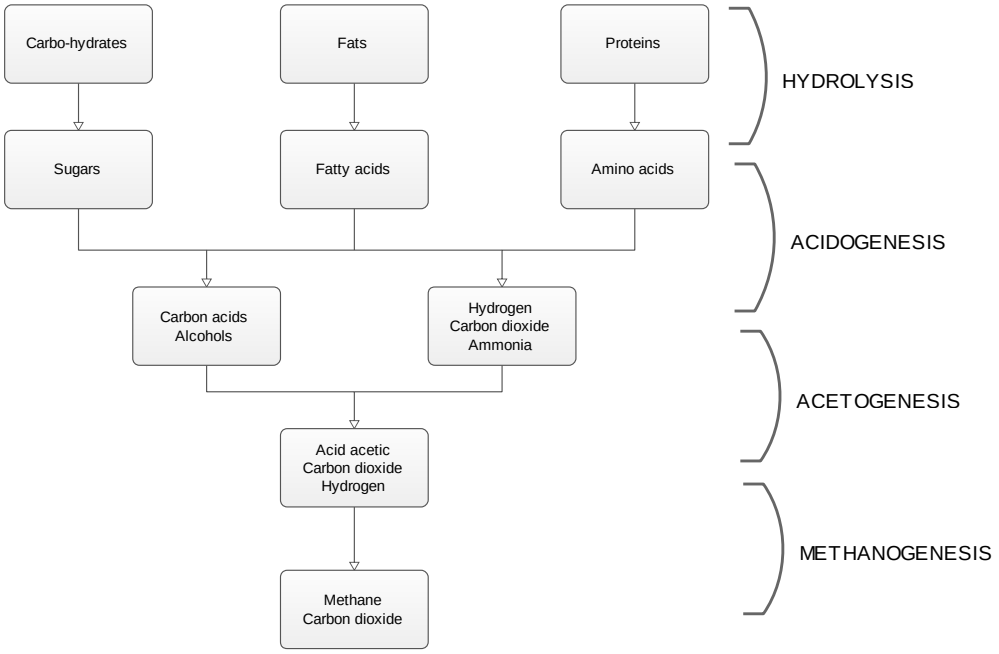


*Figure 1. Simplified diagram of the anaerobic digestion process.*

In the digester tank the steps quoted in *Figure 1* run parallel in time and space. The slowest reaction of the chain determines the speed of the total decomposition process. Hydrolysis is the speed determining process in biogas plants which process vegetable substrates containing cellulose, hemi-cellulose and lignin. Biogas production reaches its peak during methanogenesis although during hydrolysis relatively small amounts of biogas are produced [14].

The different reactions (hydrolysis, acidogenesis, acetogenesis, methanogenesis) involved in the process are described below.

*Hydrolysis*

To initiate digestion, it is necessary for complex organic matter (polymers) to cross a cell wall, in which hydrolytic agents act as extracellular enzymes that convert the polymeric matter into soluble organic compounds (mono- and oligomers)

During hydrolysis, polymers like carbohydrates, lipids, proteins and nucleic acids are converted to glucose, glycerol purines and pyridines. Hydrolytic enzymes are excreted by hydrolytic microorganisms, converting biopolymers into simpler and soluble compounds as it is shown in *Figure 2*.

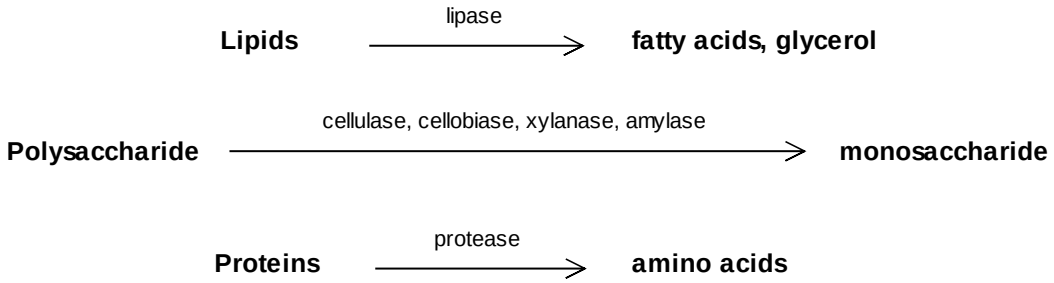


*Figure 2. Hydrolysis reactions.*

The microorganisms involved decompose the products resulted from hydrolysis and use it for their own metabolic processes.

It is one of the most careful stages, since it is generally affected by external factors such as pH, the biochemical composition of the substrate, temperature, etc.

*Acidogenesis*

In this step, the soluble molecules are converted into compounds that are subsequently used by methanogenic agents. Acetate, carbon dioxide and hydrogen (70%) as well as volatile fatty acids (VFA) and alcohols (30%) are produced by degradation of simple sugars, amino acids and fatty acids. At this stage, any trace of oxygen is also removed in the digestion process.

*Acetogenesis*

During acetogenesis, methanogenic bacteria convert products from acidogenesis, which cannot be directly converted to methane, into methanogenic substrates. Methanogenic substrates like acetate, hydrogen and carbon are the oxidation products of VFA, with carbon chains longer than two units, and alcohols, with carbon chains longer than one unit. The production of hydrogen inhibits the metabolism of the acetogenic bacteria and can be regarded as a "waste product" of acetogenesis. In the methanogenesis step, hydrogen is converted into methane. As symbiosis of two groups of organisms acetogenesis and methanogenesis usually run parallel.

*Methanogenesis*

Methanogenic bacteria act on the previous compounds and complement the anaerobic digestion process with the production of methane. The equations are presented in *Figure 3*: 70% of the methane produced in the biodigester results from the decarbolixation of the acetic substance since only two bacteria are able to use the acetate, while the remaining 30% is produced from conversion of hydrogen and carbon dioxide.

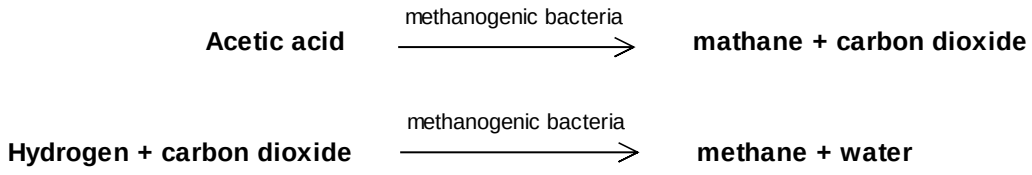


*Figure 3. Methanogenesis reactions.*

These reactions should be carried out in controlled environments since the efficiency of anaerobic digestion is influenced by some critical parameters, thus it is crucial that appropriate conditions for anaerobic microorganisms are provided. Exclusion of oxygen, constant temperature, pH-value, nutrient supply, stirring intensity as well as presence and amount of inhibitors (e.g. ammonia) have a strong influence on the growth and activity of anaerobic microorganisms. The methane bacteria Methane need to strictly avoid the presence of oxygen in the digestion process.

Methane formation takes place within a relatively narrow pH interval, from about 5,5 to 8,5, with an optimum interval between 7,0-8,0 for most methanogens. The anaerobic digestion (AD) process can take place at different temperatures, divided into three temperature ranges: psychrophilic (below 25ºC), mesophilic (25ºC – 45ºC), and thermophilic (45ºC – 70ºC). In practice, the operation temperature is chosen with consideration to the feedstock used and the necessary process temperature is usually provided by floor or wall heating systems, inside the digester.

### *Alternative methods of biogas production*

#### *Integration of pyrolysis and anaerobic digestion*

Pyrolysis combined with anaerobic digestion is one way to optimize biomass utilization and produce higher quality biogas (mainly $CH_4$). These processes are in the investigation stage.

In the pyrolysis process, heat is applied without adding oxygen in order to generate from biomass (lignocellulosic biomass, industrial and municipal solid waste, lignite and digestate) pyrolysis gas composed mainly of CO, $H_2$ and $CO_2$ and the minor components are others gases ($CH_4$ and some volatile impurities). The main advantage of

this process is that relatively dry and slowly biodegradable biomass such as wood or wood chips not suitable for the AD process, can be converted into pyrolysis gas.

The integrated pyrolysis and anaerobic digestion, involves the thermochemical conversion of the digestate and the bioconversion of the pyrolysis liquors. HÜBNER, et al. (2015) [15] showed that aqueous pyrolysis liquors from digestate pyrolysis can be converted to biogas without any additives and by unadapted inoculum.

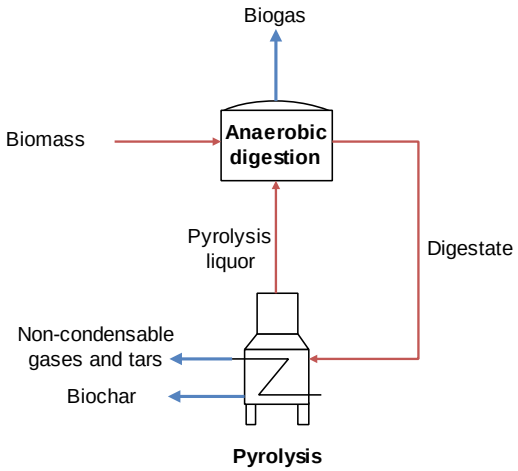


*Figure 4. Integrated pyrolysis and anaerobic digestion process, using pyrolysis liquor as a carbon source.*

Another alternative for the integration of pyrolysis with anaerobic digestion is to use the pyrolysis gases as a carbon source. LI, et al. (2017) [16] proved that the gas-liquid mass transfer is the limitation for the biomethanization of the pyrolysis gas and that this can be improved with mixing, as well as the addition of $H_2$ to the anaerobic reactor, it can transform the pyrolysis gas into biogas of high quality (91.1% $CH_4$).

### *1.2.2* Biogas upgrading and purification

As previously mentioned, biogas has different applications, for which impurities must be removed as they can produce undesirable effects. The effects of each pollutants are summarized below [5,17,18].

- $CO_2$: Decreasing calorific value, anti-knock properties of engines, corrosion.
- $H_2O$: Corrosion due to reaction with $H_2S$, $NH_3$, and $CO_2$ to form acids. Damage due to formation of condensate and ice. Accumulation of water in pipes.

- $H_2S$: Corrosion, emissions and toxic to health. $SO_2$ and $SO_3$ are formed due to combustion and cause corrosion with water and are more toxic than $H_2S$.
- $NO_2$: NOx Emissions, anti-knock properties of engines, corrosion when dissolved in water.
- $O_2$/air: Explosive mixtures due to high concentrations of $O_2$ in biogas.
- $Cl^-$: Corrosion in combustion engines.
- $F^-$: Corrosion in combustion engines.
- Dust: Clogging due to deposition in compressors and gas storage tanks.
- Hydrocarbons: Corrosion in engines due to combustion.
- Siloxanes: Formation of $SiO_2$ and microcrystalline quartz due to combustion; deposition at spark plugs, valves, and cylinder heads abrading the surface.

Each of the applications has different purity requirements or specifications. In addition to one country to another these specifications may vary. *Tables 2 and 3* show general composition guidelines for different biogas uses, and requirements for injection in to the natural gas in different countries, respectively [19-22].

*Table 2. General guidelines for impurities removal for biogas application.*

| Biogas use | $H_2S$ | $CO_2$ (%vol) | $H_2O$ (%vol) |
|---|---|---|---|
| Gas heating (boiler) | < 250 ppm | No removal required (25-30) | No removal required (6) |
| Kitchen Stove | <10 ppm | No removal required (25-30) | No removal required (6) |
| Stationary engine (CHP*) | <1000 ppm | No removal required (25-30) | Avoid condensation (< 3) |
| Vehicle Fuel | Removal required (5 mg/m$^3$) | Recommended (< 4) | Removal required (< 3) |
| Natural Gas Grid | Removal required (5 mg/m$^3$) | Removal required (≤ 3) | Removal required (1 - 8) |

*Table 3. Biogas requirements for injection into natural gas grids.*

| Component | Sweden | France | Switzerland | Germany | Netherlands | Austria |
|---|---|---|---|---|---|---|
| $CH_4$ (% vol) | ≥97 | ≥86 | ≥96 | ≥96 | ≥85 | ≥96 |
| $CO_2$ (% vol) | ≤3 | ≤2.5 | ≤6 | ≤6 | ≤6 | ≤3 |
| $O_2$ (% vol) | ≤1 | ≤0.01 | ≤0.5 | ≤0.5 | ≤0.5 | ≤0.5 |
| $H_2$ (% vol) | ≤0.5 | ≤6 | ≤4 | ≤5 | ≤0.5 | ≤4 |
| CO (% vol) | – | ≤2 | – | – | ≤1 | – |
| $H_2S$ (mg/Nm3) | ≤10 | ≤5 | ≤5 | ≤5 | ≤5 | ≤5 |
| Total sulphur (mg/Nm3) | ≤23 | ≤30 | ≤30 | ≤30 | ≤16.5 | ≤10 |
| $NH_3$ (mg/Nm3) | ≤20 | ≤3 | ≤20 | – | ≤3 | 0 |
| $H_2O$ (mg/Nm3) | ≤3 | – | – | – | – | – |
| Heavy metals (mg/Nm3) | – | ≤1 | ≤5 | ≤5 | – | – |
| Siloxanes (mg/Nm3) | – | – | – | – | ≤5 | ≤10 |
| Halogens (mg/Nm3) | – | ≤1 (Cl) ≤10 (F) | ≤1 | 0 | ≤50/25 (Cl/F) | 0 |
| Mercaptans (mg/Nm3) | – | ≤6 | ≤5 | ≤15 | ≤6 | ≤6 |

As seen in *Tables 2 and 3*, the specifications for each use are different, but in general terms hydrogen sulfide needs to be removed regardless of use, while in the case of $CO_2$ or $H_2O$, removal is necessary in some applications. We can also see that for a particular biogas application (injection into natural gas grids) the specifications vary from country to country.

### *1.2.3 Upgrading technologies*

To achieve the quality specifications of each application, the biogas must be subjected to upgrading and pre-upgrading treatments. The technologies currently developed for the biogas upgrading include adsorption, absorption (physical and chemical), membrane separation, and cryogenic. A Classification of these upgrading technologies is shown in *Figure 5*.

Biogas upgrading technologies can be classified into two groups: the physical and chemical methods and the biological methods. The latter are still in the research and development stage and are not yet available on a commercial scale.

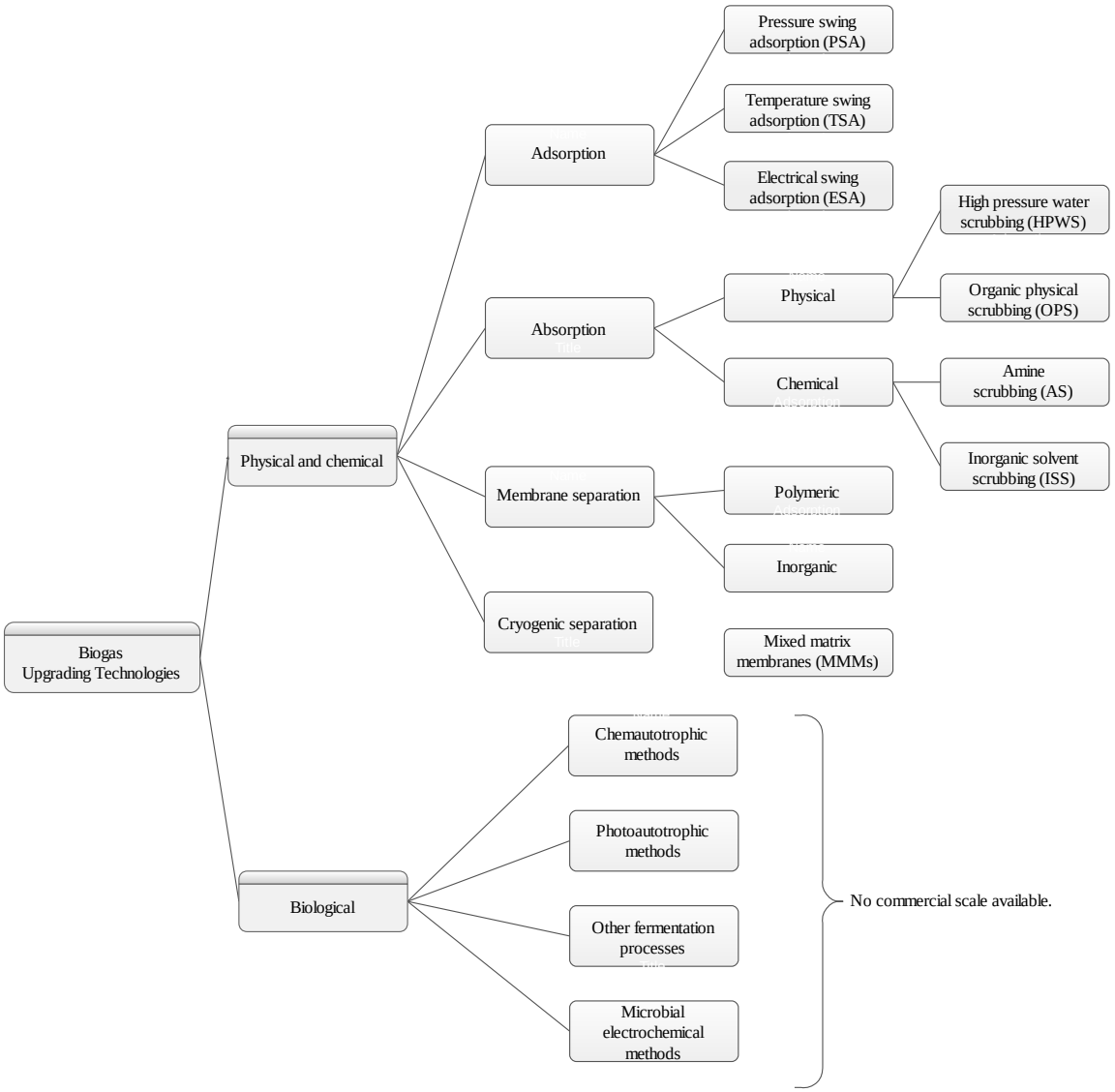


*Figure 5: Classification of biogas upgrading technologies*

Within the physical and chemical technologies group are four types: adsorption, absorption, membrane separation and cryogenic separation. In the second group we have biological technologies. The technologies summarized in *Figure 5* are described below.

## Physical and chemical technologies

### *Adsorption*

The adsorption process is based on the ability of certain solids to selectively adsorb, according to molecular size, a solute from a gas stream. Therefore a mass

transfer occurs from the gas stream to the surface of the adsorbent material and is due to physical or Van der Waals forces.

*Pressure swing adsorption (PSA)* process is a high pressure adsorption where undesirable gases such as $CO_2$ are separated from biogas, and then the pressure is reduced to desorb the adsorbed gases [23,24]. In this method, $H_2S$ must be removed before adsorption since it is considered toxic for the process and its adsorption is irreversible [25].

*Temperature swing adsorption (TSA)* is an adsorption process that occurs at constant pressure, and thermal energy is required to regenerate the adsorbent, therefore this process will be a good option when a cheap energy source is available [26,27].

*Electrical swing adsorption (ESA)* is another method in which the regeneration of the adsorbent takes place by passing electricity through the saturated adsorbent, the heat generated by the Joule effect facilitates the removal of $CO_2$ [28]. While this method reduces the cost of $CO_2$ capture, electrical conductivity is required for the adsorbent used [2].

***Absorption***

The absorption process is a separation process based on the solubility differences of various gaseous components in a particular liquid solvent. The biogas stream meets a liquid stream that flows counter-current in a packed column to increase the contact area between the liquid and the gas. In biogas upgrading, carbon dioxide is the absorbed component, since it is more soluble than methane, therefore the gas stream leaving the column has a high concentration of methane [2].

*Physical absorption*

In physical absorption is performed at low temperatures by the formation of Van der Waals forces between adsorbate and adsorbent. The solvent capacity increases nearly linearly with pressure following Henry's law, and the solvent is regenerated by reducing the pressure,

*High pressure water scrubbing (HPWS):* Since $CO_2$ and $H_2S$ are more soluble in $H_2O$ than $CH_4$, high pressure water scrubbing (HPWS) is one of the most common and well known technology used to remove these gases from biogas. Biogas is fed into the

bottom of a packed column while water is fed counter-currently with an operating pressure of 10 bar [29]. Henry's law rules the physical absorption of the gases, its states that at a constant temperature, the amount of any dissolved gas is directly proportional to its partial pressure in the gas stream. Additionally, at low temperature solubility of $CO_2$ can be increased [30].

*Organic physical scrubbing (OPS)* has the same principle as water scrubbing, but it uses an organic solvent instead of water. Various organic solvents such as methanol (CH3OH), N-methyl pyrrolidone (NMP), and polyethylene glycol ethers (PEG) are used to absorb $CO_2$. Due the solubility of $CO_2$ is higher in in these solvents than in water organic solvent demand and pumping requirement are lower [21, 31]. In this absorption process $H_2S$, $H_2O$, $O_2$, $N_2$, and halogenated hydrocarbons are also removed together with $CO_2$, but the prior removal of $H_2S$ is recommended. The operating pressure is 6–8 bar [32].

*Chemical absorption*

Chemisorption occurs when chemical interactions like covalent bonds are formed between adsorbate and the solid surface of the adsorbent. Chemisorption can occur even at very low concentrations, and the chemisorbed species are not easily desorbed under ambient temperature conditions.

*Chemical amine scrubbing (AS):* Chemical absorption involves reversible reaction between absorbed substances and solvent. The amine scrubber process takes place in an absorber, where the $CO_2$ is absorbed from the biogas and after that, a stripper which separates the $CO_2$ from the waste amine solution by heating under reduced pressure [33]. The raw biogas and the amine solution circulate in counter current flow, entering the gas through the bottom. The $CO_2$ in the biogas reacts with the amine solution and is absorbed. This is an exothermic reaction, which increases the temperature of the absorber from 20–40 to 45–65°C [34]. Usually, the solubility of $CO_2$ in $H_2O$ increases with decreasing temperature [30] but in amine scrubbing (AS), the reaction rate between $CO_2$ and the amine solution increases with increasing temperature, subsequently gives more absorption of $CO_2$. The operating pressure of the absorber is 1–2 bar. The principal disadvantages of this process are: the technology requires prior removal of $H_2S$ and treat waste chemicals; corrosion, and contaminant build-up which makes the process more complex [2].

*Inorganic solvent scrubbing (ISS)* generally employs an aqueous solution of alkaline salts such as sodium, potassium, ammonium, and calcium hydroxides [35]. The absorption of $CO_2$ in this alkaline solution is assisted by agitation. The turbulence in the solvent and the contact time between biogas and liquid increase the diffusion of the $CO_2$ in the solvent [21].

***Membrane separation***

In this process a membrane works as a permeable barrier through which specific compounds pass differently and control their permeability based on the applied driving forces, such as the difference in concentration, pressure, temperature and electrical charges of different species. Two models are used to explain the membrane separation process, such as the solution diffusion model and the pore flow [36]. In the first one, permeates are dissolved in the membrane material, thereafter they diffuse through the membrane due to the difference in concentration. Finally, the permeates are separated by convective flow driven by pressure through small pores [37]. In biogas upgrading, $CO_2$ penetrates through the membrane while $CH_4$ is retained on the inlet side as retained. Membrane gas separation is most beneficial when the gas flow is low and the input $CO_2$ content is high [38]. This is a cheap process that includes low capital and operating costs, less energy demand and requires the installation of simple and compact membrane equipment [39]. For biogas purification, the three types of membrane used are Polymeric, Inorganic and Mixed Matrix Membranes (MMM). The prior removal of $H_2S$ from the raw biogas is necessary because it can adversely affect the performance of the membrane.

*Polymeric membranes* are economically competitive in biogas upgrading and separation compared to conventional technologies in both capital and operating costs [20]. However, the investigation of polymeric materials for gas separation has been questioned due to the upper limit of compensation between permeability and selectivity. In fact, highly permeable membranes tend to have low selectivity [40].

*Inorganic membranes* offer more mechanical strength, thermal stability, and resistance against any chemical compared to conventional polymeric membrane. For the most part, inorganic membranes facilitate permeability and selectivity. The fabrication these membranes is a stringent process and requires continuous monitoring due to their fragile structure [36,41,42].

*Mixed matrix membranes: b*oth polymeric and inorganic membranes have limitations that motivate researchers to develop new membranes. Developments so far focus on the integration of inorganic and polymeric membranes known as mixed matrix membranes (MMMs). Significant improvement in MMMs properties is expected due to superior inorganic particle separation performance combined with high processability and moderate processing cost of base polymer membranes [43,44].

***Cryogenic separation (CS)***

This process takes advantage of the fact that various gases such as $CO_2$ and $H_2S$ liquefy under different pressure and temperature conditions. It operates at very low temperature (−170 ° C) and high pressure (80 bar). The boiling point of $CH_4$ at 1 atm is −161.5 ° C, while the boiling point of $CO_2$, which is −78.2 ° C, and therefore allows the separation of $CO_2$ from $CH_4$ when liquefied [45]. These operating conditions are maintained using a series of compressors and heat exchangers [46]. This separation is considered as a new technology, which is still under development [17,30], but some commercial plants are already in operation [17]. This separation can be useful if the objective is to produce liquefied biomethane (LBM) and liquid natural gas (LNG) [47]. Pre-separation of $H_2O$ and $H_2S$ is necessary to avoid clogging of the equipment due to freezing of the water in the raw biogas [19].

**Biological technologies**

Biological technologies are mainly classified as chemoautotrophic and photosynthetic. Most of these configurations have been experimentally tested and are in an early stage of pilot or full-scale implementation. The main advantage of such technologies is related to the fact that $CO_2$ is converted into other energy-containing or high value-added products under moderate operating conditions (i.e. atmospheric pressure, moderate operation temperature) that contribute significantly to development bio-based sustainable and circular economy [1].

***Chemautotrophic methods***

The chemoautotrophic biogas upgrading methods are based on the action of hydrogenotrophic methanogens that can utilize $H_2$ to convert $CO_2$ to $CH_4$ based on the following equation [1]:

$4H_2 + CO_2 \rightarrow CH_4 + H_2O \qquad \Delta G = -130.7 KJ/mol$

However, the $H_2$ required in the reaction must be derived from a renewable source, in order to make the biological upgrading a renewable method. Solar and wind energy are the most attractive options for this method, but these are point energy sources that need damping to supply energy when it is dark and the wind is still there [1]. The batteries used for storing electricity still have several drawbacks such as the low capacity to store large amounts of electricity and the high cost of production. Electrolysis of water using renewable electricity separates the water into $O_2$ and $H_2$. In this way, $H_2$ generation, which is an energy carrier in itself, is a clean energy source free of $CO_2$ emissions. However, $H_2$ has the inherent disadvantage of very low volumetric energy density, which makes it difficult to store [48] and therefore practical application is also difficult. Therefore, the integration of this technology for the conversion of $H_2$ to $CH_4$ is very attractive, since it integrates wind or solar energy technology with biogas technology. This process is a promising means of converting electricity into a carrier of chemical energy, which can be easily stored in existing natural gas infrastructure [1].

***Photoautotrophic methods***

The improvement of photosynthetic biogas is an alternative method to sequester $CO_2$, in order to obtain a gas rich in $CH_4$. Recovery of methane from photo-autotrophic technologies can achieve up to approximately a 97% probability of the type of reactor and the selected algae species. This biotechnological process is catalyzed by phototrophic organisms such as algae in enclosed or open photobioreactors. In the updating process, the biogas is injected directly into the photobioreactor or externally into an absorption column where the microalgae broth stream is recirculated from the main tank. Subsequently, photoautotrophic microorganisms, such as prokaryotic cyanobacteria or eukaryotic microalgae, can efficiently absorb $CO_2$, using solar irradiation, water and nutrients to produce biomass, oxygen and heat. The elimination of $H_2S$ is very important to increase the sustainability of the process [1].

***Other fermentation processes***

Although $CO_2$ in biogas can be biologically converted to methane with the addition of $H_2$ to achieve biogas upgrading, the production of valuable liquid products (e.g. acetate, ethanol, butyrate, butanol, etc.) from $CO_2$ in biogas is more attractive [49,50] since biogas upgrading by conversion of $CO_2$ in biogas together with $H_2$ has the inherent challenge that needs availability of cheap $H_2$ sources [1].

***Microbial electrochemical methods***

In a microbial electrolysis cell, the electrons released by bacteria from the oxidation of organic compounds on the anode can combine with protons to generate hydrogen in the cathode chamber [51,52]. Hydrogen formed at the cathode can be used for biogas enhancement. In fact, Cheng et al. (2009) [53] reported for the first time that methane could be produced directly by reducing $CO_2$ at the cathode using a biocathode in MEC, and methane was produced with an overall energy efficiency of 80%, providing potential technology for improvement of biogas. Later, it was also shown that the reduction of $CO_2$ to methane was attributed both to extracellular transfer of electrons and to abiotic hydrogen produced (electrolysis of water), which depended on the established potential of the cathode [54]. However, most current research is based on laboratory scale experiments; the technical and economic limitations for expanding this technology for biogas improvement remain to be explored [1].

### *1.2.4* Advantages and disadvantages of biogas upgrading technologies

Biological upgrading technologies have lower technical requirements compared to available technologies, reducing operating and investment costs and energy [55]. They give a high final volume of $CH_4$ [48]. It does not involve $CH_4$ emissions to the atmosphere, resulting in improved environmental benefits for the life cycle [56]. It converts excess electricity to $CH_4$, which is easily transported and distributed over long distances for various uses, such as heating, cogeneration generation, and vehicle fuel [48]. Despite the fact that the biological upgrading technology has several advantages, this technology could only be the best alternative to the traditional biogas upgrade process when electricity is surplus and $H_2$ is cheaper. Therefore, these limitations must be addressed to introduce your business application [2].

The adsorption processes TSA requires thermal energy to regenerate the adsorbent material, while PSA uses compression energy. Therefore, TSA is the best option when the energy resource is economical. At ESA, regeneration is carried out by passing electricity through the saturated adsorbent and the heat generated by the Joule effect facilitates the release of $CO_2$ [28]. Although this process reduces the cost of $CO_2$ capture compared to TSA and PSA, electrical conductivity is required for the absorbent used. The *Table 4* summarizes the general advantages and disadvantages of biogas upgrading techniques [2].

*Table 4.Advantages and disadvantages of different biogas upgrading technologies.*

| Technology | Advantages | Disadvantages |
|---|---|---|
| **PSA** | High $CH_4$ concentration (95–99% )[20]<br>The humidity of the raw biogas can be removed [24]<br>Less energy demand with low emissions, [32]<br>Clean and water-free gas [47]<br>Fast and easy installation[57] | High capital investment and operational costs (due to a number of columns in PSA unit) [20]<br>Previous $H_2S$ and water elimination steps are needed [24, 30]<br>Susceptible to fouling by impurities in the biogas stream [47]<br>Possible high $CH_4$ losses by valves malfunction [57] |
| **HPWS** | High CH4 concentration (>97% )[20]<br>No previous $H_2S$ step is needed H2S [32]<br>No special handling and chemicals are required [47]<br>Easy operation with low $CH_4$ loses (< 2%) [19]<br>Regeneration of water is possible [58] | High investment and operating costs [20,32]<br>Less efficient [47]<br>Slow process [45]<br>High pressure, need higher energy [17]<br>Requires large amounts of water [58]<br>Corrosion problem [59] |
| **OPS** | CH4 concentration (>97% ) [20]<br>Remove organic components such as $H_2S$, $NH_3$, HCN, and $H_2O$ [47]<br>Low $CH_4$ loss [57] | Complex operation with high investment and operational costs [20]<br>Uneconomical for small-scale applications [47]<br>Need high energy to regenerate the solvent [57]<br>Solvent is expensive and difficult to handle [60]<br>Solvent regeneration is difficult if H2S is not removed first [61] |
| **CSP** | CH4 concentration (>99% ), low operational costs [20]<br>Complete H2S removal - operation at low pressure [32]<br>High selectivity for CO2- low CH4 loss [47] | High investment and regeneration of solvent cost [20,32,62]<br>Problems of contaminant build-up, corrosion, and amine breakdown[47]<br>Waste chemical requires treatment [17] |
| **MS** | Less operational and capital investment costs and high $CH_4$ recovery up to>96% [20]<br>Small space requirements and available at low capacities [60,63].<br>Low maintenance cost [64]<br>Simple and environmentally friendly process [65]<br>Easy operation [66]<br>Fast and easy installation [32]<br>Highly reliable and cheap process [67] | For high purity product, multiple steps of membrane are required [20]<br>Low $CH_4$ yield in single step [22]<br>Not suitable for high purity needs [60]<br>Consumes more electricity per unit of gas produced [45] |
| **CS** | High purity of CH4 with 98% concentration [17]<br>Low energy and cost is required to obtain highly pure liquefied biomethane and very low $CH_4$ loss (1% ) [68]<br>Eco-friendly process [69] | High investment, maintenance and operational costs [68]<br>High $CO_2$ purity and high energy requirements [45]<br>Use of different expensive process equipment [58] |

The biogas upgrading technologies that are most used today are membrane separation, pressure swing adsorption, washing with water and washing with amines [63,70,71]. In the face of the various upgrading techniques with their advantages and disadvantages and permanent innovations, adsorption technology, specifically pressure swing adsorption PSA, continues to be one of the most convenient making a cost-efficiency balance.

### *1.2.5 Pressure swing adsorption (PSA)*

This technology is based on the separation of the different biogas gases based on their molecular characteristics and the affinity of the adsorbent material. The principle of PSA technology is the properties of pressurized gases to attract solid surfaces. Therefore, at high pressure, large amounts of gas will be absorbed, while a decrease in pressure will result in gas release. The PSA process can be divided into a four steps *Figure 6*, called adsorption, blow-down, purge, and pressurization [71]. The first step is the injection of the compressed biogas (4–10 bar) into an adsorption column, in which the adsorbent material will selectively retain $CO_2$, $N_2$, $O_2$ and $H_2O$ while methane flows through the column and It can be collected from the top by decreasing the pressure. In practice, generally four adsorption columns are installed to ensure the maintenance of a continuous operation [58]. Once the adsorbent is saturated, the gas stream will continue to the next column. In the saturated column, the adsorbent material will be regenerated by a desorption process, in which the pressure decreases and the trapped gases are released. The gas mixture that is released from the columns contains significant amounts of methane and therefore must be recycled leading to the PSA inlet [70]. $H_2S$ must be removed before the biogas is injected into the PSA column since $H_2S$ adsorption is normally irreversible [32]. This method is advantageous because the equipment is compact, requires a low cost of investment of energy and capital, and finally, due to its safety and simplicity of operation [72]. Crude biogas can be upgraded to 96-98% methane concentration; however, up to 4% methane can be lost within the exhaust gas stream [63,17].

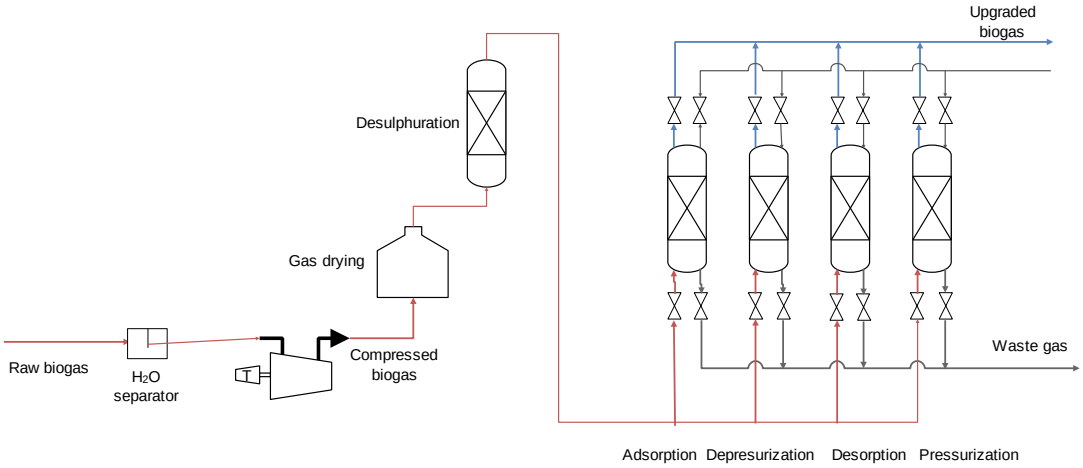


*Figure 6. Flowsheet of PSA*

### *1.2.6* Adsorbents for PSA technology

In the PSA process, adsorbent materials play a fundamental role, so their proper selection is very important to achieve a high selectivity of $CO_2$. The most commonly used adsorbents for biogas upgrading are organic framework adsorbents zeolites and activated carbon [32,74]. The pores of these adsorbents are responsible for the easy penetration of $CO_2$ while retaining the $CH_4$ molecules. This is due to the different sizes of the $CO_2$ and $CH_4$ molecules and also to their adsorption capacity [75,76].

Adsorption of carbon dioxide through physical adsorbents (carbonaceous and non-carbonaceous materials) has a low energy demand compared to chemical adsorbents. The reason is that no new bonds are generated between the carbon dioxide and the surface of the adsorbent, which generates less energy demand for the regeneration of the adsorbent. However, well-known physical adsorbents such as activated carbon have the disadvantage of low carbon dioxide-nitrogen selectivity, and successfully overcoming this problem will dominate amine absorption technologies and save energy [76]. Zeolites show good selectivity for carbon dioxide; however they suffer from low $CO_2$ loading in humid conditions. In general, the design of new adsorbent materials with good stability, high affinity for $CO_2$, acceptable scalability, and low energy requirements are the main research activities for solid adsorbents for biogas upgrading. *Figure 7* shows the most common adsorbents used in carbon dioxide capture [74].

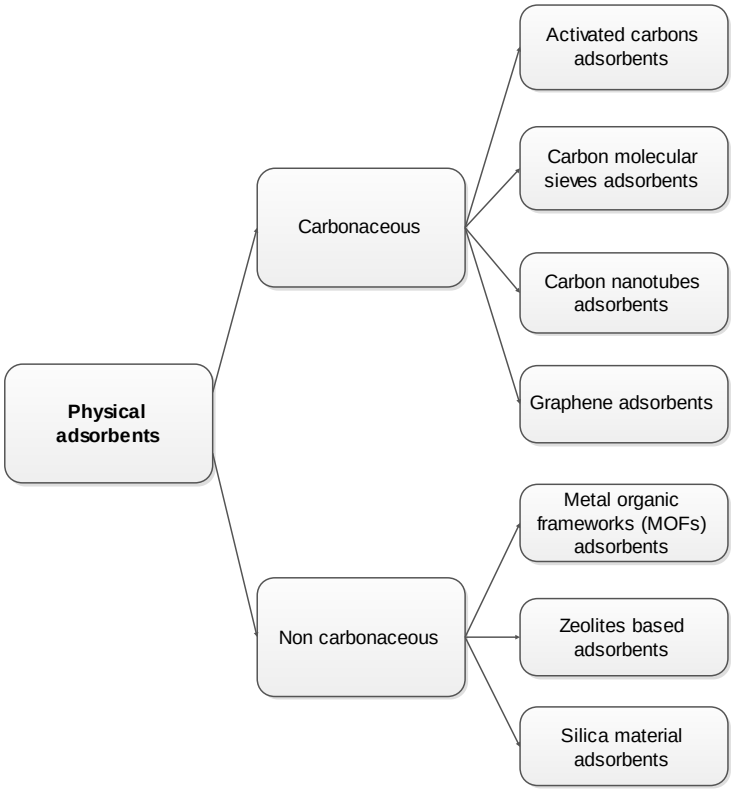


*Figure 7. Physical solid adsorbents for carbon dioxide adsorption*

When carbon dioxide molecules reach the electronic environment of the adsorbing surface they will achieve reduced free energy. The interactions of gas-solid surface molecules and the associated reduction in entropy increases the number of $CO_2$ molecules on the adsorbent surface. Adsorption can be physical, governed by Van der Waals forces, or it can be chemical, involving the formation of a chemical bond between the adsorbent surface and the adsorbate. Various materials describe the representation of different chemisorption mechanisms in the adsorption process. For example, for MOFs adsorbents, the mechanism of the chemical reaction exists through uncoordinated metal sites, and functional groups are formed on the surface of MOFs, while for biomass adsorbents, the interaction process exists by intermolecular forces [77]. Carbon dioxide adsorption can exist with or without the consistency of chemical bonds. For carbon dioxide fisisorption, the quadrupole momentum-electric field electric field gradient interaction often dominates carbon dioxide interactions with the adsorbent surface. While, the number of trapped gas molecules increases as the temperature decreases due to the exothermic nature of the adsorption process. The temperature and pressure of operation are important parameters in the control of the process since they

strongly influence the adsorbed molecules. The International Union of Pure and Applied Chemistry defined three types of adsorbents based on pore size as 1) 2nm micropores, 2) 2 to 50nm mesopores, 3) 50nm macropores. [74]

The adsorbent material selected for carbon dioxide removal must meet certain requirements to be competitive economically and operationally [74]:

- High adsorption performance is important as it minimizes both the amount of adsorbent and the size of the process equipment. Adsorption can be considered competitive against other existing technologies, when the process achieves a carbon dioxide load in a range of 3-4 mmol / g of adsorbent [78].
- Selectivity is defined as the ratio of the carbon dioxide capacity to another gas capacity that has a direct impact on the trapped carbon dioxide. A competitive adsorbent must show high selectivity for carbon dioxide, as well as offer high CO2 capacity in wet conditions.
- Adsorbents must have rapid adsorption-regeneration kinetics for carbon dioxide. Since it controls the cycle time. The carbon dioxide adsorption kinetics in the porous adsorbents influenced by the reaction kinetics of the carbon dioxide with the functional group on the adsorbent surface and by the mass transfer through the adsorbent surface.
- The mechanical resistance of the adsorbent is crucial to maintain high kinetics.
- The adsorption heat is the measure of the energy required for the regeneration of adsorbents it should be as low as possible. For fission cases, the heat of adsorption varies between -25 and -50 kJ/mol, while between -60 and -90 kJ/mol for chemisorption [79].
- Finally, the cost of the adsorbent is the main characteristic.

### *Adsorbent materials classification*

- ***Carbonaceous materials adsorbents***

The carbonaceous materials consisting mainly of carbon and other materials associated with excellent properties such as eco-affinity, thermal and chemical stability,

high resistance, thermal and electrical conductivity [80, 81]. They are also inexpensive, are obtained from natural sources, have a high specific surface area, large volume of pores and light weight. These materials are available in different classes such as porous activated carbons, carbon molecular sieve, carbon nanotubes, and graphene [74].

*Activated carbon materials (ACs)*

ACs are efficient adsorbents in $CO_2$ removal due to their high specific surface area, which gives them a high adsorption capacity. As a general description, activated carbon adsorbents have the advantages of low regeneration energy, easy to regenerate, low regeneration temperature, availability of raw materials and high thermal stability. On the other hand, CA materials are soft and can cause high bed wear and more adsorbent replacement. The adsorption performance improves when the partial pressure of carbon dioxide increases [82]. While the adsorption capacity decreases as the partial pressure of carbon dioxide decreases due to the impact of the presence of impurities such as NOx, SOx, $H_2O$ and Hg0 [83,84].

*Carbon molecular sieves adsorbents*

Carbon molecular sieves adsorbents are a special member of microporous carbon adsorbents with molecule-sized pores. These adsorbents were reported to have the same or more adsorption capacity than other carbon-based adsorbents [85]. Carbon molecular sieve adsorbents are considered promising adsorbents and may improve the selection of carbon dioxide over methane, which merits further study [74].

*Carbon nanotube adsorbents*

Carbon nanotube materials are a new member of the carbon group that attracted great attention as a new type of adsorbent as they can act as an efficient adsorbent for carbon dioxide removal. Carbon nanotubes are efficient thermal conductors and exhibit unique electrical properties, making them potentially useful in a wide variety of technological applications [86, 87]. Especially along their long axes, individually, they show a remarkable electrical conductivity that approximates the typical values of metals [85, 86]. Carbon nanotubes also demonstrate unique thermal characteristics [90, 91]. Its thermal conductivity is approximately double that of diamond [92]. Carbon nanotube materials are a promising adsorbent for carbon dioxide [74].

*Graphene*

Graphene is a new class of carbonaceous materials with acceptable adsorption capacity that have recently received massive attention. Basically it is a flat single layer of $sp^2$ hybridized carbon atoms, densely packed in an ordered two-dimensional honeycomb network. Since 2012, many research papers [93-95] have been offered to investigate the use of graphene-graphite as a carbon dioxide adsorbent due to the large active surface area and low preparation cost. The investigation of graphenes as adsorbents for the elimination of $CO_2$, has pending challenges to improve the adsorption rate and selectivity for $CO_2$ [74].

- ***Non-carbonaceous dry adsorbents***

*Metal organic framework adsorbents*

Organometallic Structure Materials (MOFs) are a new group of solid adsorbent materials produced by the combination of metal ions linked by coordination bonds. Due to the flexibility of handling both metal ions and organic bonds, numerous options are presented to manage the pore size, shape and potential of the adsorption surface, which improves selectivity, $CO_2$ loading and kinetics adsorption-desorption. The field of MOFs materials is still emerging, many investigations look for the possibility of the development of new adsorbents. These structures have a high capacity to adsorb carbon dioxide at high pressures, although at atmospheric pressures, their adsorption capacity is less compared to other physical adsorbents [74, 96, 97].

*Zeolites*

Zeolites are microporous crystalline framework materials that exist naturally but also can be synthesized in the laboratory. They consist of a chain of channels to capture gas molecules with regular pore sizes ranging from 0.5 to 1.2 nm [98]. Therefore, they have been widely used in gas separation technologies. Zeolites have been extensively studied for carbon dioxide removal in the interest of their impact on molecular sieving and robust dipole-quadrupole (electrostatic) interactions between carbon dioxide and alkali metal cations in zeolite frameworks [99]. The carbon dioxide removal performance of zeolite adsorbents is strongly affected by operating temperature and

pressure. They have high regeneration temperatures close to 573K, therefore the regeneration of carbon dioxide becomes a great loss of energy [100].

*Silica materials*

Silica-based materials are another group of dry non-carbonaceous adsorbents for $CO_2$ capture that have a large surface area, a large pore size and great mechanical stability [101]. Silica is generally the support on which other materials are added for the removal of carbon dioxide. There is a wide range of silica-based adsorbents and recent studies seek the development of mesoporous silica materials for effective carbon dioxide removal [102-104]. Modification of mesoporous silica-based materials with amines can efficiently improve $CO_2$ adsorption capacity because primary and secondary amines have a high affinity for carbon dioxide [105]. Research aims to create silica compounds synthesized with adsorbent amines that can increase the surface area and result in a compatible pore size for carbon dioxide molecules [74].

***Adsorbent materials comparison***

A comparison of the adsorbent materials mentioned above is shown in *Table 5*. It can be said that MOFs adsorbents are more compatible and suitable with respect to the adsorption capacity of carbon dioxide, but they carry a higher cost. On the other hand, these adsorbents are generally unstable in a humid environment. As seen in *Table 5*, carbon dioxide has a low selectivity in zeolite adsorbents, moderate in carbon-based absorbents, high in adsorbents of organometallic structures [74, 106].

*Table 5. Comparison of physical solid adsorbents for carbon dioxide adsorption.*

| Feature | Carbon based adsorbents | Zeolites adsorbents | Metal organic frameworks adsorbents |
|---|---|---|---|
| **Major exercise** | High pressure $CO_2$ adsorption | $H_2$ enrichment | $CO_2$ separation |
| **$CO_2$ selectivity** | Medium | Low | High |
| **Adsorption Capacity** | Higher than zeolite at high pressure and decrease at low pressure. | Medium | High |
| **Stability under humid conditions** | Stable | Unstable | Unstable |
| **Synthesis cost** | Acceptable cost | Low cost | Expensive |
| **Advantages** | -High conductivity<br>-High stability<br>-Large surface area and pore volume<br>-light weight | -Large micro-mesopores<br>-Medium CO2 uptake at ambient conditions<br>-Low energy penalty<br>-Relatively fixed pore size<br>-Great potential as a supported thin-film membrane in dehydration and isomer separation. | -Flexible pore size<br>-High surface area<br>-Low adsorption and regeneration temperatures<br>-Activation by solvent removal (drying) at T < 100 °C.<br>-Great potential as a mixed matrix membrane. |
| **Disadvantages** | -Low adsorption and regeneration temperatures<br>-Low adsorption capacity in comparison to other types of zeolites and MOFs | -High affinity with water ▪ High energy penalty ▪ Difficult readiness<br>-Activation is by calcination | -Low $CO_2$ loading at low pressures<br>-Low economic efficiency<br>-Difficult synthesizing processes<br>-Sensitive to humid<br>-Deployment at high temperature can destroy the construction of MOFs |

### *1.2.7* Simple mathematical models for the Adsorption Process

To describe the dynamic behavior of an adsorption column, the concentration vs. time profile called breakthrough curve must be found, a correct estimation of this profile is essential for a successful design and scaling of any adsorption process. Among the most used and discussed models in the recent literature are the Bohart-Adams model, the Tomas model and the Yoon-Nelson model. There are also innumerable comparisons between these three models where their settings are compared in each particular case. In a recent study, the CHU, Khim Hoong (2020) [107] has shown that these three models are essentially the same, the three models respond to a logistic equation with small differences in the definitions of the parameters of each of them, but the mathematical essence is the same in the three models. These similarities and differences are detailed in *Chapter 2*. Since these three models are essentially the same, we focus in this work on the Bohart-Adams model, the oldest of them all. Starting from simple models, the design and scaling process of biogas upgrading will also be simple, less time-consuming and more economical.

# *Chapter 2* – MATHEMATICAL MODELING AND SIMULATION

## 2.1 Introduction

This chapter introduces the Bohart-Adams equation, the assumptions that this equation entails and therefore its field of validity, explains its similarity with the Yoon Nelson and Tomas models. Finally, the ways to estimate the parameters for this model applied to the purification and upgrading of biogas are explained. The criteria used for the escalation process are also introduced.

## 2.2 Mathematical modeling and simulation

The Batch-adsorption occurs in a closed system containing a desired amount of adsorbent contacting with a certain volume of adsorbate solution, while fixed-bed adsorption usually occurs in an open system where adsorbate solution continuously passes through a column packed with adsorbent [11]. The dynamic behavior of a fixed bed column is described in terms of the effluent concentration–time profile, i.e., the breakthrough curve. The shape of this curve is determined by the shape of the equilibrium isotherm and influenced by the individual transport processes in the column and adsorbent [108].

For column adsorption, the way how the breakthrough curve is determined is a very important issue because it provides the basic but predominant information for the design of the column adsorption system. Without the information of the breakthrough curve one cannot determine a rational scale of a column adsorption for practical application. There are two widely used approaches to obtain the breakthrough curve of a given adsorption system: direct experimentation or mathematical modeling. The experimental method could provide a direct and concise breakthrough curve of a given system. However, it is usually a time-consuming and economical undesirable process, particularly for the trace contaminants and long residence time. Also, it greatly depends upon the experimental conditions, such as ambient temperature and residence time. Comparatively, mathematical modeling is simple and readily realized with no experimental apparatus required, and thus, it has attracted increasing interest in the past decades [11].

The general way to predict the breakthrough curve is to solve a set of partial differential equations which consist of a macroscopic mass conservation equation,

uptake rate equation (sometimes including a set of equations), and isotherm equation, together with a set of initial and boundary conditions.

Considering the different components of the adsorption systems (solvents, adsorbate, adsorbent), variable operation conditions and specific demands of accuracy and calculative simplicity, it is an important but challenging task to propose a general use model, because typically a model derived from particular assumptions is only suitable for very limited situations, being less accurate then applied in a more general setting [11].

Finally, with a good estimate of the breakthrough curve through mathematical modeling, the adsorption process can be simulated, to predict the behavior of the system, security problems and ensure the normal operation.

### 2.3 Mathematical modeling and simulation in adsorption

The starting point for developing a mathematical model is the differential mass balance equation system: for an element in the adsorption column and for the adsorbent particle within that element. Considering an element of the bed, through which flows a stream with a fluid concentration c (z, 1) of the adsorbable specie. If the flow stream can be represented as an axially dispersed plug flow, the transient gas phase component mass balance is:

$$-D_L\frac{\partial^2 c}{\partial z^2}+\frac{\partial}{\partial z}(vc)+\frac{\partial c}{\partial t}+\left(\frac{1-\epsilon}{\epsilon}\right)\frac{\partial \overline{q}}{\partial t}=0 \qquad \textit{(Eq.1)}$$

where, c is the concentration of the adsorbable specie, $D_L$ axial dispersion coefficient, q is the sorbate concentration in the adsorbent, $\overline{q}$ value of q averaged over crystal and pellets, z the distance measured from the column inlet, $v$ interstitial velocity of fluid, $\epsilon$ voidage of adsorbent bed and t denotes time. This equation includes the axial dispersion term, convection flow term, accumulation in the fluid phase, and source term caused by the adsorption process on the adsorbent particles [109].

The mass balance for an adsorbent particle produces the expression for adsorption rate and can be written:

$$\frac{\partial \overline{q}}{\partial t}=f(q,c) \qquad \text{(Eq. 2)}$$

The expression of mass transfer rate, write as a single equation, is commonly a set of equations comprising one or more diffusion equations with associated boundary conditions. The dynamic response of the column is given by the solution (c (z, t), $\overline{q}$ (z, t)) to *Equations (1)* and *(2)* subject to the initial and boundary conditions imposed on the column. A disturbance in the inlet composition involves a mass transfer zone or concentration front that propagates through the column with a characteristic velocity determined by the equilibrium isotherm. To determine the form of the concentration front *Equations (1)* and *(2)* must be solved simultaneously and the location of the front at any time can be found simply from a total mass balance [109].

From *Equations 1* and *2* derive the mathematical models that have been developed until now. With different simplifications and assumptions according to the classification of the system [108]. This classification is detailed below to understand these assumptions in general guidelines.

### *I. Nature of the equilibrium relationship*

*Linear isotherm.* The system presents a dispersive behavior. For the step or pulse response analytical solutions can generally be found.

*Favorable isotherm.* The concentration front approaches the constant pattern form. Analytical solutions for the constant pattern asymptotic profile is easy to obtain, but for the lead curve or pulse response an analytical solution is only possible in some special cases.

*Unfavorable isotherm.* The system presents a dispersive behavior. Most commonly observed during desorption of a favorably adsorbed species. Analytical solutions are rarely possible.

### *II. Isothermal or Near Isothermal*

*Isothermal.* The resistance to heat transfer can be neglected. The extension of the concentration front is entirely due to axial dispersion and resistance to mass transfer. This situation usually occurs in a chromatographic system with a low concentration of the adsorbable component.

*Near Isothermal.* The heat transfer between the fluid and the solid is slow enough to modify the concentration front. This situation usually occurs in chromatographic

systems when the adsorbable species has a high heat of adsorption or is present at a relatively high concentration level.

### *III. Concentration level of adsorbable components*

*Trace systems.* The adsorbable component is present only at low concentration in an inert vehicle. The velocity is considered constant, since changes in the velocity of the fluid through the mass transfer zone are negligible.

*Nontrace Systems.* Adsorbable species are present at concentration levels high enough to cause significant variation in fluid velocity through the mass transfer zone. This effect occurs mainly in gases.

### *IV. Flow model*

*Plug flow.* Axial dispersion is neglected so that the term $-D_L\frac{\partial^2 c}{\partial z^2}$ can be released, reducing the *equation 1* to a first order hyperbolic equation.

*Dispersed plug flow.* Axial dispersion is significant, so the $-D_L\frac{\partial^2 c}{\partial z^2}$ must be kept in the *equation 1*.

### *V. Complexity of the kinetic model*

*Negligible mass transfer resistance*. Instantaneous equilibrium is assumed at all points in the column.

*Single mass transfer resistance.* (i) Expression of linear rate:

$$\frac{\partial \bar{q}}{\partial t} = k(q^* - q) \; or \; k'(c - c^*) \qquad \textit{(Eq.3)}$$

where $q^*$is the equilibrium value of $q$ and $c^*$ is the equilibrium value of $c$. The rate coefficient is an effective global mass transfer coefficient (grouped parameter). (ii) Diffusion model: The dominant resistance to mass transfer is intraparticle diffusion, which is described by the diffusion equation with associated boundary conditions.

*Two mass transfer resistors*. i) External resistance of the fluid film plus intraparticle diffusion. (ii) Two internal diffusion resistances (macropore-micropores).

*Three mass transfer resistors.* External film resistor plus two intraparticle diffusion resistors (macropore-micropore) [109].

In this work, plug flow systems will be considered, therefore in *equation 1*, the term $-D_L \frac{\partial^2 c}{\partial z^2}$ is neglected, so the general equation of mass balance in the fluid can be rewritten:

$$\frac{\partial}{\partial z}(vc) + \frac{\partial c}{\partial t} + \left(\frac{1-\epsilon}{\epsilon}\right)\frac{\partial \bar{q}}{\partial t} = 0 \qquad \textit{(Eq. 4)}$$

With these concepts defined, we are in position to extend in the mathematical model on which the present work focuses; the century-old Bohart-Adams model. This model, which is one hundred years old, continues to be used and discussed in many works even today. This is due to the B-A model has a highly sought-after potential, this is its mathematical simplicity, which allows obtaining the breakthrough curve easily and in short times.

## 2.4 The Bohart-Adams model

Bohart and Adams (1920) came up with a model, later called the Bohart-Adams (B-A) model, when they proceeded with their work of analyzing the typical chlorinecharcoal transmission curve. They hypothesized that the uptake rate of chlorine is proportional to the concentration of the chlorine existing in the bulk fluid and the residual adsorptive capacity of charcoal [110].

Bohart and Adams model [110] was proposed to describe adsorption of one component. How this model consider a plug flow and trace system, the changes in the velocity of the fluid through the mass transfer zone and the dispersion axial term are negligible, thus the velocity is considered constant and the flux unidirectional. Hence, the mass balance equation from which it starts is:

$$v\frac{\partial C}{\partial z} + \frac{\partial c}{\partial t} + \left(\frac{1-\epsilon}{\epsilon}\right)\frac{\partial \bar{q}}{\partial t} = 0 \qquad \textit{(Eq. 5)}$$

In this model it is assumed that the sorbate-adsorbent interaction can be represented by the following quasi-chemical rate expression:

$$\frac{\partial \mathrm{q}}{\partial \mathrm{t}} = \mathrm{k_{BA}C}(q_0 - q) \qquad \textit{(Eq. 6)}$$

where $q_0$ is the sorption capacity and $k_{BA}$ is the Bohart-Adams kinetic constant [11].

This rate equation implies that at equilibrium ($\frac{\partial \mathrm{q}}{\partial \mathrm{t}}$ = 0). *Equation 5* reduces to an irreversible or rectangular equilibrium relationship between the bulk solution and adsorbent, this means, the component adsorbed onto the adsorbent surface cannot be desorbed [12]. ( *Figure 8).*

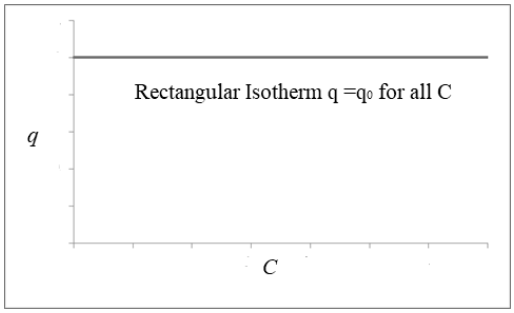


*Figure 8. Equilibrium sorption irreversible (or rectangular) isotherm [5].*

Neglecting axial dispersion, the analytical solution to *Equations 5 and 6* derived by Bohart and Adams [110] is given by

$$\frac{C}{C_0} = \frac{\exp(\alpha)}{\exp(\alpha) + \exp(\beta) - 1} \qquad \textit{(Eq. 7)}$$

with $\alpha = K_{BA}C_0\left(t - \frac{z}{v}\right)$ and $\beta = \frac{K_{BA}\rho_p q_0 Z}{v}\left(\frac{1-\epsilon}{\epsilon}\right)$, where $\rho_p$ is the apparent adsorbent density.

*Equation 7* can be converted to the commonly quoted form of the Bohart–Adams model applying two simplifications [111].

1. The two exponential terms $\exp(\alpha)$ and $\exp(\beta)$ are usually much greater than 1, so the "1" term on the right-side of *Eq. 7* can be disregarded.
2. Because of sorption the time needed for the sorbate to exit the column is far longer than the time needed for the bulk solution to flow from the column inlet to the outlet, which is given by Z/v. We can therefore assume that t is much longer Z/v and

disregard the Z/v term in the expression for $\alpha$. These two approximations simplify *Eq. 7* to

$$\frac{C_0}{C}\exp(K_{BA}C_0 t) = \exp(K_{BA}C_0 t) + \exp\left(\frac{K_{BA}\rho_p q_0 Z}{v}\left(\frac{1-\epsilon}{\epsilon}\right)\right) \qquad \textit{(Eq. 8)}$$

Dividing each term of *Eq. 8* by $\exp(K_{BA}C_0 t)$ and taking the natural logarithm of each side gives

$$\ln\left(\frac{C_0}{C}-1\right) = \frac{K_{BA}\rho_p q_0 Z(1-\epsilon)}{v\epsilon} - K_{BA}C_0 t \qquad \textit{(Eq. 9)}$$

Then, combining $\rho_p q_0(1-\epsilon)$ as a single entity:

$$\rho_p q_0(1-\epsilon) = \left[\frac{\text{adsorbent mass}}{\text{adsorbent volume}}\right]\left[\frac{\text{sorbate mass}}{\text{adsorbent mass}}\right]\left[\frac{\text{adsorbent volume}}{\text{bed volume}}\right]$$

$$\rho_p q_0(1-\epsilon) = \left[\frac{\text{sorbate mass}}{\text{bed volume}}\right]$$

In the above expression can be seen that $\rho_p q_0(1-\epsilon)$ is formally identical to the sorption capacity per unit volume of the bed, $N_0$. The entity $v\epsilon$ is equivalent to the superficial velocity $u$. So replacing $\rho_p q_0(1-\epsilon)$ and $v\epsilon$ in Eq. 9 with $N_0$ and $u$, the linear form of the Bohart- Adams expression is obtained [11].

$$\ln\left(\frac{C_0}{C}-1\right) = \frac{K_{BA}N_0 Z}{u} - K_{BA}C_0 t \qquad \textit{(Eq. 10)}$$

Rearranged the terms of the *Equation 10*, the expression of the breakthrough curve of the Bohart-Adams model is the obtained.

$$\frac{C}{C_0} = \frac{1}{1+\exp\left(\frac{K_{BA}N_0 Z}{u} - K_{BA}C_0 t\right)} \qquad \textit{(Eq.11)}$$

### *2.4.1* Validity of the Bohart-Adams model

In a recent study, Chu (2020) [107] performs an analysis of the two forms of the B-A equation that we can find in the literature, the two forms are comparable with the equations of exponential population growth one, and logistic population growth the other. The starting point of these two forms is the same, but the exponential equation

has more simplifications than the logistics one. The analytical solution for the adsorbate outlet concentration as a function of time could be given by

$$\frac{C}{C_0} = \frac{\exp\left[K_{BA}C_0\left(t - \frac{\epsilon Z}{u}\right)\right]}{\exp\left(\frac{K_{BA}N_0Z}{u}\right) + \exp\left[K_{BA}C_0\left(t - \frac{\epsilon Z}{u}\right)\right] - 1}, \qquad \textit{(Eq.12)}$$

with $\frac{C}{C_0} = 0$ for $0 < t < \frac{\epsilon Z}{u}$, where, $\epsilon Z/u$ is the residence time. *Equation 13* was first given by Amundson [112], and is a more rigorous version of the original solution derived by Bohart and Adams [109]. The E*quation 12* could be rewritten as

$$\ln\left(\frac{C_0}{C} - 1\right) = \ln\left[exp\left(\frac{K_{BA}N_0Z}{u}\right) - 1\right] - K_{BA}C_0\mathrm{t}\left(t - \frac{\epsilon Z}{u}\right) \qquad \textit{(Eq. 13)}$$

Normally, term $exp\left(\frac{K_{BA}N_0Z}{u}\right)$ is much larger than unity and t is much bigger than $\epsilon Z/u$ , the unity term and the $\epsilon Z/u$ term of *Equation 13* can be neglected. The resulting is:

$$\ln\left(\frac{C_0}{C} - 1\right) = \frac{K_{BA}N_0Z}{u} - K_{BA}C_0t \qquad \textit{(Eq. 14)}$$

which is identical to Equation 10, the linear form of the Bohart-Adams model [107].

Neglecting the unity term in the left-hand member of *Equation 14*, the second liner form of the Bohart-Adams model is obtained

$$\ln\left(\frac{C_0}{C}\right) = \frac{K_{BA}N_0Z}{u} - K_{BA}C_0t \qquad \textit{(Eq. 15)}$$

*The graph of Equation 14* results in the graph of a logistic function while *Equation 15* is an exponential function [107].

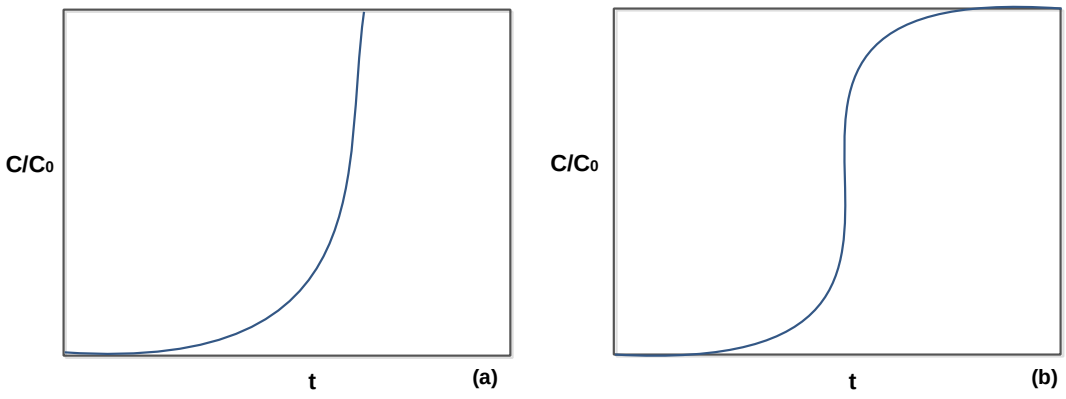


*Figure 9. Mathematical forms of Bohart-Adams model Eq. 15 (a) and Eq.14 (b)*

*Figure 9* shows that *Equation 15* gives a J-shaped curve while *Equation 14* gives an *S*-shaped or sigmoidal curve. As an exponential function, *Equation 15* predicts that breakthrough percentage increases without bound with time. Whereas, *Equation 14* shows the main feature of the logistic equation: exit concentration approaches an upper asymptotic value of unity with time [107].

Both curves give a good fit for advance values less than 15%, for higher advance values *Equation 14* is superior in adjustment [107]. This is because its first users designed it to adjust small advance values [113]. Finally, *Equation 15* does not represent simplifications practices and rarely prove to be superior to *Equation 14* [107].

Chu (2020) [107], also makes a comparison between the Bohart-Adams, Thomas and Yoon-Nelson models, showing that the three models are mathematically equivalent. The three models respond to the following logistic equation.

$$\ln\left(\frac{C_0}{C}-1\right)=a-bt \qquad \textit{(Eq. 16)}$$

*Table 6. Parameters a and b of the B-A, T, and Y-N models expressed in terms of the logistic equation.*

| Model | a | b |
|---|---|---|
| Bohart-Adams | $K_{BA}N_0Z/u$ | $K_{BA}C_0$ |
| Thomas | $K_Tq_0M/Q$ | $K_TC_0$ |
| Yoon-Nelson | $K_{YN}\tau$ | $K_{YN}$ |

Where $K_T$ is the Thomas rate coefficient, $q_0$ is the solid loading per unit mass of adsorbent (governed by the Langmuir isotherm), M is the mass of adsorbent, and Q is the volumetric flow rate, $K_{YN}$ is the Yoon-Nelson rate coefficient and $\tau$ is the time required for 50% breakthrough [107].

The three models, B-A, Thomas, and Yoon-Nelson can all be expressed in terms of the logistic function with two general parameters, *a* and *b*. Then, it only takes to fit the logistic equation to breakthrough data to extract the two global parameters, from which the specific parameters of the three models can be calculated. Mathematically they are one and the same, and will therefore give similar fit quality [107].

In another study, Chu (2010) [12] shows that the main difference between the Bohart-Adam and Thomas model is the isotherm assumed. The Tomas model assumes a Langmuir isotherm while the Bohart-Adams, assumes a rectangular isotherm. The

difference between the two isotherms is presented in *Figure 10*. So, when the isotherm is highly favorable for sorption, the Thomas model will give results that are very similar to those obtained from the Bohart–Adams model. The Bohart–Adams model can thus be regarded as a limiting form of the Thomas model.

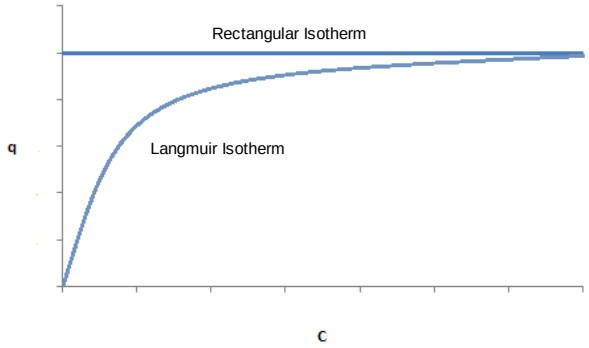


*Figure 10. Rectangular Isotherm and Langmuir Isotherm.*

This confirms that the Bohart-Adams model, despite its mathematical simplicity, has a very large adjustment potential comparable to the also widely used models of Tomas and Yoon-Nelson.

### *2.4.2* Parameter estimation of the Bohart-Adams model

In this work, two ways of estimating the parameters were used. The first one using the linear form of the Bohart-Adams model *Equation 10*, plotting ln(Co/C−1) against t, $K_{BA}$ can be evaluated from the slope of the graph and $N_0$ from the *y*-intercept. It is only necessary to fit the logistic function (*Equation 15*) to a given set of breakthrough data once to extract *a* and *b* from the resultant plot. With known values of *a* and *b* and other relevant operational and system variables, the $N_0$ and $K_{BA}$ parameters can be computed from the relations given in *Table 6*.

The second way is calculate the stoichiometric time, fixing it in the diagram and determine by error estimate the $K_{BA}$ parameter so as to fit with the experimental breakthrough data. Reordering *Equation 11*, is obtained

$$\frac{C}{C_0} = \frac{1}{1 + \exp\left[K_{BA}C_0\left(\frac{N_0 Z}{C_0 u} - t\right)\right]} \qquad \textit{(Eq. 17)}$$

In other hand, the amount adsorbed at equilibrium can be written as [114]

$$q^* = \frac{F_0 C_0}{M} \int_0^\infty \left(1 - \frac{y_{i,e}}{y_{i,0}}\right) dt \qquad \textit{(Eq.18)}$$

where $F_0$ is total volumetric flow rate, $y_0$ and $y_e$ are the initial and effluent of the adsorbable component "*i*", W is the mass of adsorbent.

A useful quantity to use based on *Equation 18* is the stoichiometric time $t_s$, which is given by

$$t_s = \int_0^\infty \left(1 - \frac{y_{i,e}}{y_{i,0}}\right) dt \qquad \textit{(Eq.19)}$$

Malek et al. [115] showed that due to the significant velocity difference between the inlet and exit of the column in nontrace systems, *Equation 19* could give incorrect estimations of the equilibrium adsorption data. So, they proposed an expression of the stoichiometric time, which give good estimations of the stoichiometric time when the feed concentration of the adsorbable component larger than 20%.

$$t_s = \int_0^\infty \left(1 - \frac{y_{i,e}(1 - y_{i,0})}{y_{i,0}(1 - y_{i,e})}\right) dt \qquad \textit{(Eq. 20)}$$

Considering that $q_0 M = N_0 Z A$ where A is the bed cross sectional area, and $F_0 = Au$. We can rewrite *Equation 17* as

$$\frac{C}{C_0} = \frac{1}{1 + \exp[K_{BA} C_0 (t_s - t)]} \qquad \textit{(Eq.21)}$$

With this form of the Bohart-Adams equation, the parameters are estimated with stoichiometric time.

## 2.5 Mathematical modeling and scale-up applied to biogas purification and upgrading

As mentioned in the previous chapter, the composition of the biogas depends on the raw material and the type of digester, and for each particular use of biogas, specific compositions are required. In the purification and upgrading of biogas, the concentrations of impurities are adjusted to meet the specifications required for each use, if we refer to *Table 1* in the previous chapter, we can see in broad strokes that the adsorption processes of the impurities of the Biogas, since these impurities are found in very small concentrations, they would correspond to the Trace System. However when we look at $CO_2$ concentrations vary between 24-50% and according with a recent study [114] these concentrations for $CO_2$ adsorption are considered within the Nontrace System and in this cases is important to consider velocity variations when modelling fixed bed adsorption columns to accurately calculate the $CO_2$ breakthrough behavior. That studio showed that should be considered variable velocity through the bed for correctly describing $CO_2$ capture in activated carbon, crystalline bulk CuBTC MOF and pelleted CuBTC MOF, unless a very diluted feed is considered (with $CO_2$ concentration <1%). The effect of a high-pressure drop was not considered. Also shows the error in the estimation of the total amount adsorbed is practically independent of the total flow rate or the adsorbent used, but strongly dependent on the feed concentration [114].

Malek et al. [115] suggested that the correction for variable velocity should be implemented when the feed concentration is higher than 20% for light adsorbing gases (methane and ethane on activated carbon) to have errors smaller than 2% in the equilibrium amount adsorbed [115]. For gases that adsorb stronger, such as $CO_2$ on activated carbon, a feed concentration of 20% results in a shift of the breakthrough time of 6%, and a deviation in the equilibrium amount adsorbed of 6%. For $CO_2$ adsorption on bulk and pelleted CuBTC, same deviations (i.e., 6%) in breakthrough curves and equilibrium amount adsorbed were observed. In other words, to estimate the breakthrough curve in $CO_2$ adsorption, we must apply the correction for speed variation.

Once the parameters of the Bohart-Adams`s equation, $K_{BA}$ and $N_{0,}$ have been determined, with them the scaling will be carried out, for which the similarity criterion will be used, that is, the following similarities will be respected:

- Geometric similarity: the relationship between the length of the column and the diameter will be kept constant.
- Kinematic similarity: the physical properties of the fluid in both columns will be kept constant to ensure the mass transfer regime. This is simply working with the same inlet gas as in the laboratory tests.
- Dynamic similarity: the linear flow velocity in the two columns will be kept constant, on a laboratory scale and on a large scale.

Also with the Bohart-Admas parameters, a new breakthrough curve will be calculated and with them the stoichiometric time and the amount of adsorbent can be determined. The next chapter shows the scaling process applied to a biogas purification plant.

# *Chapter 3* – METHODOLOGY AND EXPERIMENTAL STUDY

## 3.1 Introduction

This chapter explains the methodology used, the mathematical tests carried out in this study. The results obtained are presented, making a comparison between the adjustments and the experimental data. Finally, the scaling process is shown from the Bohart-Adams model.

## 3.2 Methodology

In this work, different forms of the Bohart-Adams equation were studied and fit tests were carried out with the sigmoid form of said equation using a correction in stoichiometric time for the speed variation. With experimental data existing in current literature [114] corresponding to $CO_2$ adsorption, on three different adsorbents (bulk activated carbon, AC), crystalline powder (bulk CuBTC metal-organic framework, MOF) and crystalline pellets (pelleted CuBTC), with three different feed concentrations: 20%, 33% and 50% of $CO_2$ in a $CO_2$ / $N_2$ mixture. The experimental data corresponds an adsorption system composed of a single fixed bed column operated at 50ºC and 1 bar.

The data was processed using Microsoft Excel Software. In Chapter II, the two ways of processing the data used in this work were mentioned, the firth one, *Method 1* , using *Equation 10*, plotting ln(Co/C−1) against t, $K_{BA}$ can be evaluated from the slope of the graph and *N*o from the *y*-intercept [107]. The second way, *Method 2*, calculated the stoichiometric time, fixing it in the diagram and determines by error estimate the $K_{BA}$ parameter so as to fit with the experimental breakthrough data. The stoichiometric time was calculated using *Equation 19*, without the correction for velocity variation and *Equation 20* [115] with the correction for variable velocity and the results were compared. The stoichiometric time was calculated using the Numerical integration method *Simpson's Rule* [116]. After that the same experimental data was compared with the modeling carried out with the equation that considers the velocity variation.

## 3.3 Experimental study

From *Figures 11 to 13*, it can be seen that, regardless of feed concentration and type of adsorbent, the adjustment by *Method 1 and 2* with the stoichiometric time equation that considers the variation of velocity give the same result. But in the adjustment by *Method 2* with the stoichiometric time equation that does not consider the velocity variation; the breakthrough curve obtained differs from the experimental data.

*Table 7* summarizes the estimated parameters a and b of method 1, the stoichiometric time calculated with *Equation 20* (with variable velocity correction) and the stoichiometric time calculated with *Equation 19* (without variable velocity correction) and the constant $K_{BA}$ Estimated by both methods, these parameters were used in the simulation of the breakthrough curve.

*Table 7. Estimated parameters with Method 1 and 2.*

| Adsorbent | | | AC | Bulk CuBTC | Pelleted CuBTC | |
|---|---|---|---|---|---|---|
| Feed Composition | 20% | a | 5,667 | 4,639 | 6,237 | C0 = 7,45 mol/m3 |
| | | b (min-1) | 0,1872 | 0,1427 | 0,1998 | |
| | | $K_{BA}$ (m3/mol min) | 0,0251 | 0,0192 | 0,0268 | |
| | | ts Eq. 20 (min) | 30,45 | 31,79 | 30,05 | |
| | | ts Eq.19 (min) | 26,98 | 30,49 | 28,59 | |
| | 33% | a | 6,777 | 5,652 | 5,477 | C0 = 12,29 mol/m3 |
| | | b (min-1) | 0,1874 | 0,1129 | 0,1397 | |
| | | $K_{BA}$ (m3/mol min) | 0,0152 | 0,00918 | 0,0113 | |
| | | ts Eq. 20 (min) | 34,91 | 49,68 | 38,91 | |
| | | ts Eq.19 (min) | 31,27 | 46,22 | 36,16 | |
| | 50% | a | 8,143 | 4,147 | 4,022 | C0 = 18,61 mol/m3 |
| | | b (min-1) | 0,1737 | 0,0599 | 0,0718 | |
| | | $K_{BA}$ (m3/mol min) | 0,0324 | 0,00321 | 0,00385 | |
| | | ts Eq. 20 (min) | 45,91 | 69,17 | 57,22 | |
| | | ts Eq.19 (min) | 41,74 | 59,86 | 46,026 | |

### *3.3.1* Bulk activated carbon, AC

The Bohart-Adams constant $K_{BA}$ obtained by the two methods is 0.0251$m^3$/mol min for 20% inlet concentration. It can be seen in *Figure 11,* that for an initial concentration of 20% $CO_2$, on Activated Carbon, a good fit of the experimental data is obtained, provided that the equation with the correction is used for the estimation of the stoichiometric time by variable velocity. Using *method 2* with the correction for variable velocity, it can be considered a good fit. If the equation is used to calculate the stoichiometric time without the velocity correction, a good fit is not obtained.

For 30% inlet concentration the Bohart-Adams parameter $K_{BA}$ obtained by the two methods is 0.0152 $m^3$/mol min. The adjustment with both *method 1* and *method 2* is acceptable, *Figure 11*, clearly using in *method 2* the correction for velocity variation for the calculation of stoichiometric time. Otherwise the adjustment is not adequate.

When the inlet concentration is 50% the Bohart-Adams parameter $K_{BA}$ obtained by the two methods is 0.0324 $m^3$/mol min.

Comparing the experimental data with those modeled using the Bohart-Adams equation by the three ways, the best adjustment obtained is with method 2 with the correction for variable velocity for the three concentrations, *Figure 11 (b*).

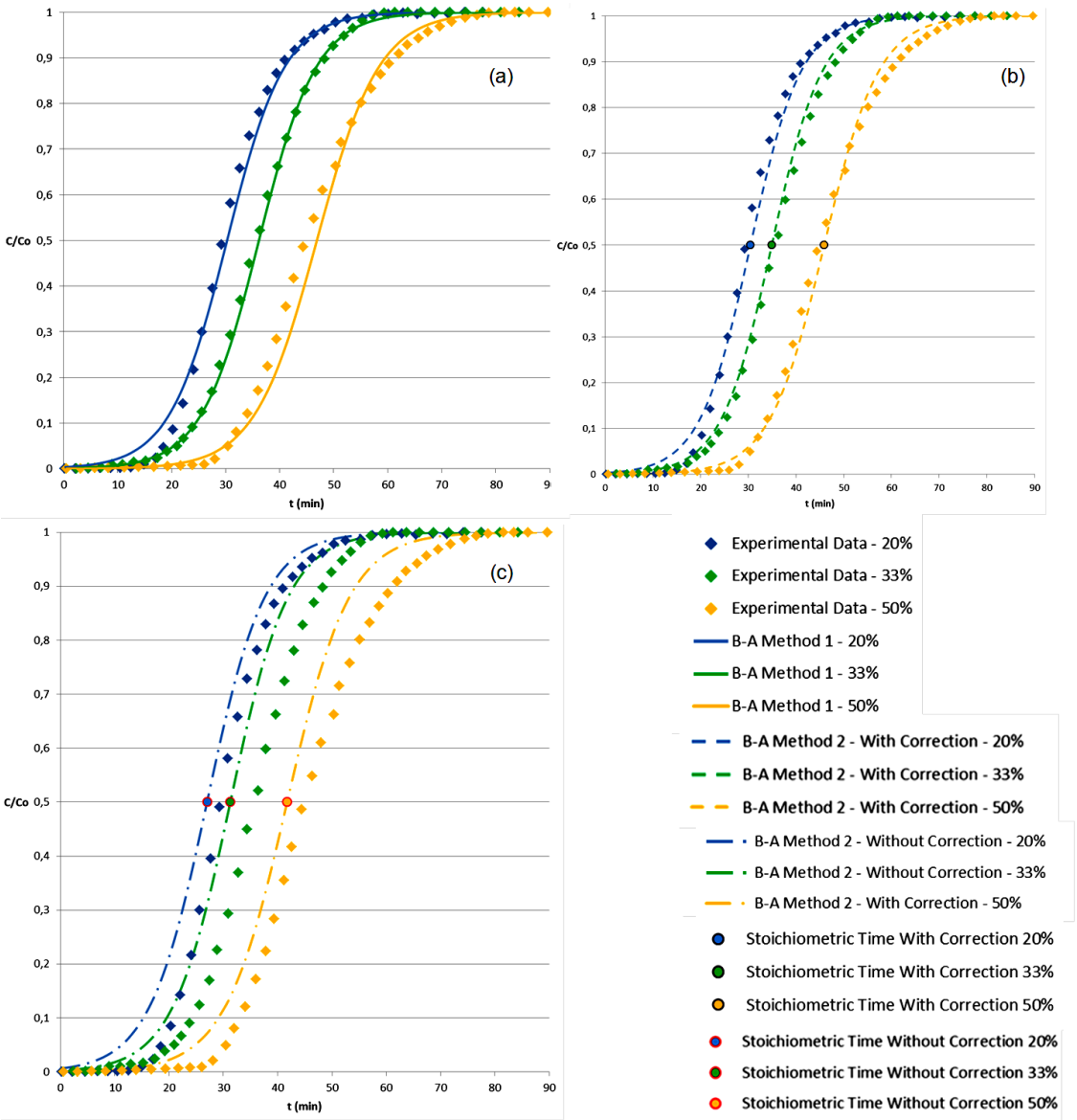


*Figure 11.Experimental data compared with Bohart-Adams model, Method 1 (a), Method 2 with the variable velocity correction (b) and Method 2 without the variable velocity correction on Bulk activated carbon, AC. (c)*

### *3.3.2* Crystalline powder, bulk CuBTC

For feed composition 20% the Bohart-Adams parameter KBA obtained by the two methods is 0.0192 m3/mol min. Figure 12 shows that for a feed concentration of 20% CO2 with bulk CuBTC as adsorbent, modeling with method 1, we can see that the two

curves follow the same trend, although there is a discrepancy in the prime values of the curve it can be considered a good fit. Now, using method 2, a better fit is observed using the stoichiometric time with the velocity correction although a discrepancy is seen in the first values (Figure 12), this discrepancy is greater when the correction for stoichiometric time is not used.

When the feed composition is 33% the Bohart-Adams parameter $K_{BA}$ obtained by the two methods is 0.00918 $m^3$/mol min. In *Figure 12* it can be seen that with bulk CuBTC as adsorbent, using *method 1 and 2* the modeled curves differ slightly from the experimental curve although both follow the same trend. Despite that difference it can be considered a good fit. This difference is even greater when calculating the stoichiometric time without speed correction, as can be seen in *Figure 12 (c).*

For feed composition 50% the Bohart-Adams parameter $K_{BA}$ obtained by the two methods is 0.00321 $m^3$/mol min. Observing *Figure 12* it can be seen that for a feed concentration of 50% $CO_2$ with bulk CuBTC the adjustments obtained with *method 1 and 2* differ slightly from the experimental data, and as expected, this difference increases with the use of the stoichiometric time without the velocity correction, *Figure 12 (c).*

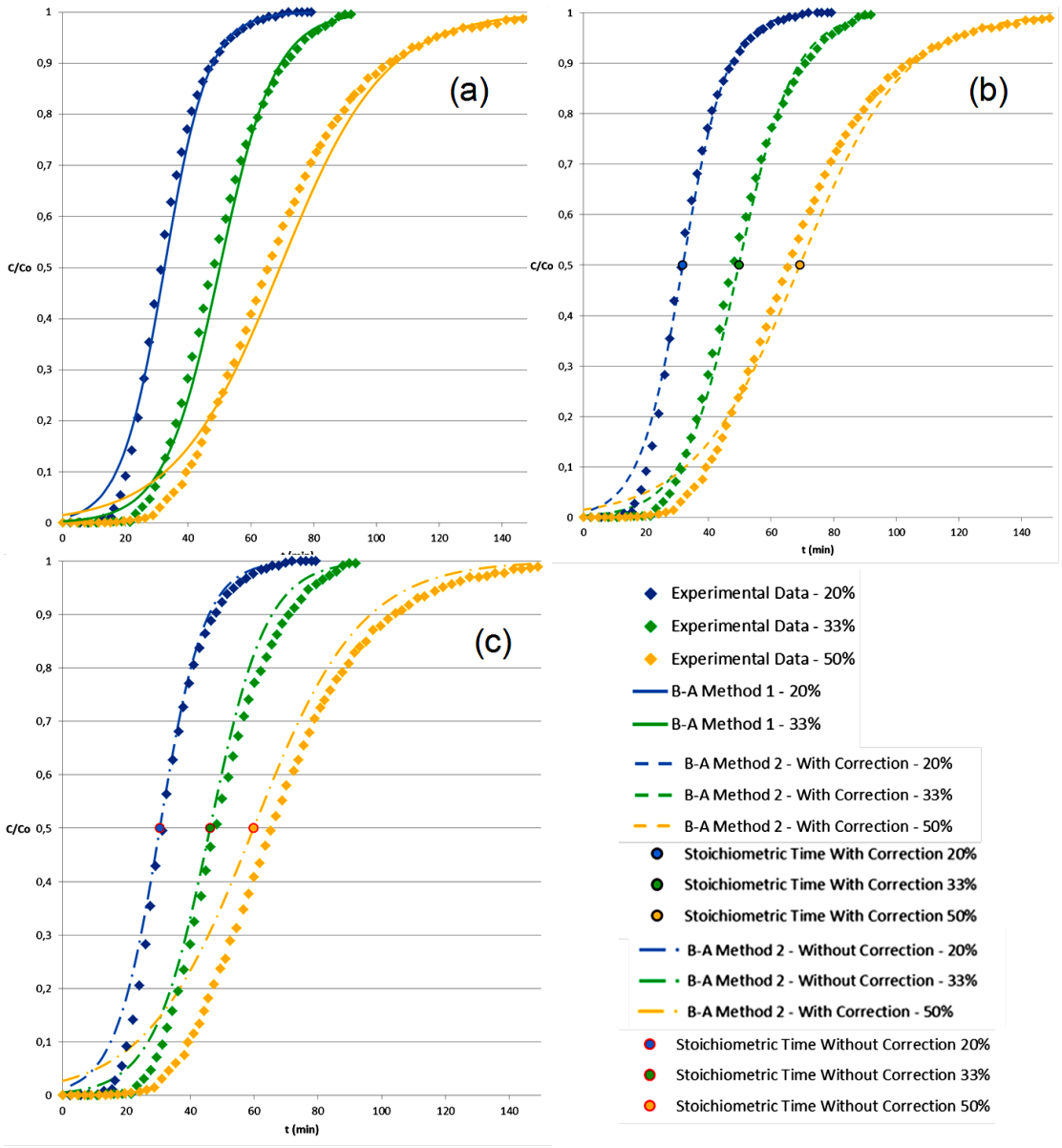


*Figure 12.Experimental data compared with Bohart-Adams model, Method 1 (a), Method 2 with the variable velocity correction (b) and Method 2 without the variable velocity correction on bulk CuBTC.(c)*

### *3.3.3* Crystalline pellets, pelleted CuBTC

For the feed composition 20% the Bohart-Adams parameter $K_{BA}$ obtained by the two methods is 0.0268 $m^3$/mol min. For the pelleted CuBTC adsorbent with an initial concentration of 20%, *Figure 13 (a)* shows that although the experimental curve and the one modeled with *method 1* follow the same trend, a small discrepancy is observed between the two curves.

*Figures 13 (b)* show that for the CuBTC pelleted adsorbent with an initial concentration of 20% of $CO_2$, *method 2* using the stoichiometric time with the variable velocity correction gives the best adjustment.

With an inlet composition 33% The Bohart-Adams parameter $K_{BA}$ obtained by the two methods is 0.0113 $m^3$/mol min. The curves modeled with *method 1 and 2* fit well with the experimental data but a well fit is given by *method 2* with the correction. If stoichiometric time is used without velocity correction, the modeled curve does not fit the experimental data *Figure 13 (c).*

With a feed concentration of 50% $CO_2$ with pelleted CuBTC the Bohart-Adams parameter $K_{BA}$ obtained by the two methods is 0.0385 $m^3$/mol min. The adjustments obtained with *method 1 and 2* differ slightly from the experimental data, as occurs with the bulk CuBTC adsorbent at the same initial concentration. It also happens that the difference between the modeled curve and the experimental data increases when the stoichiometric time is used for the calculation without speed correction *Figure 13 (c).*

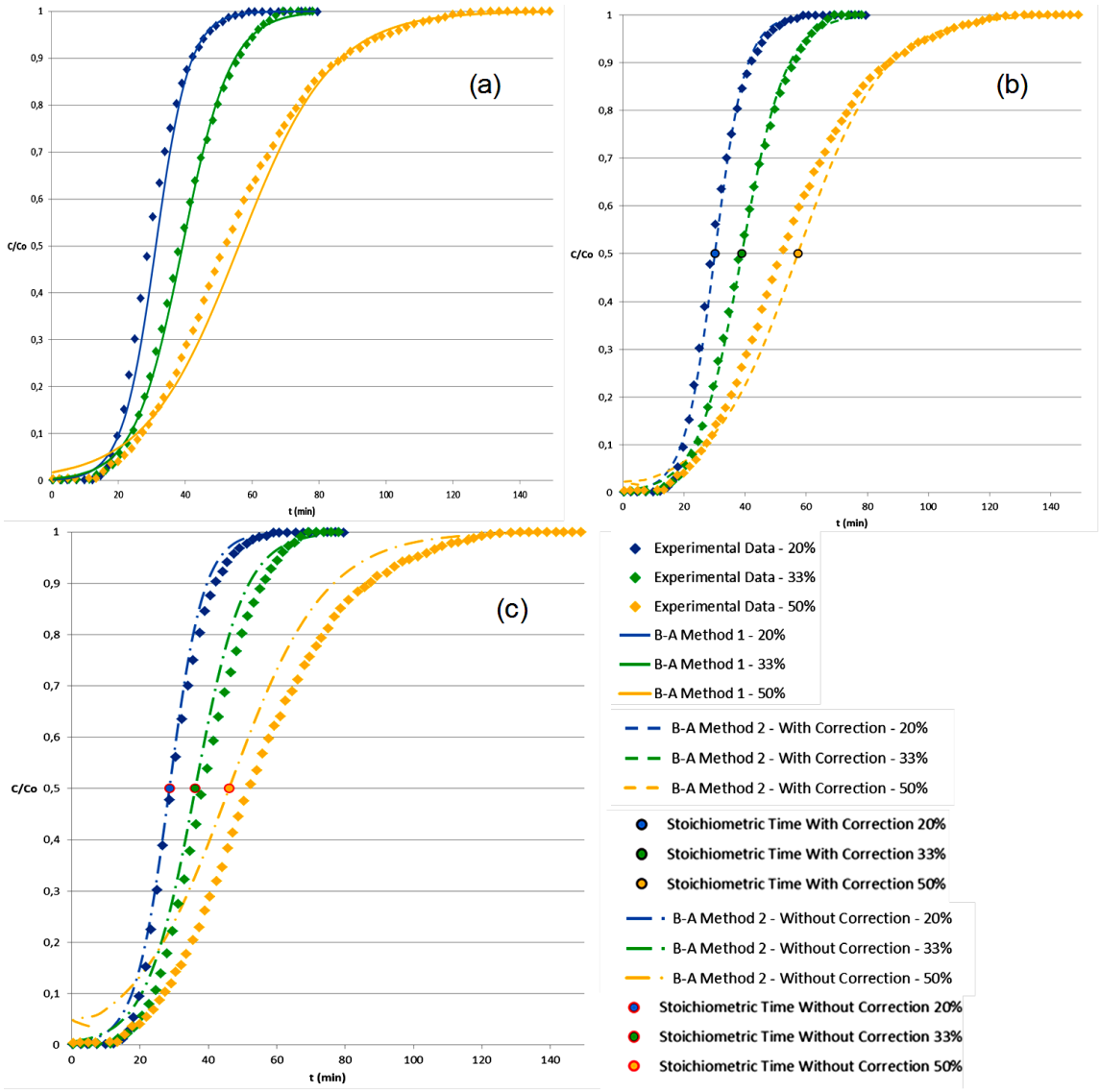


*Figure 13.Experimental data compared with Bohart-Adams model, Method 1 (a), Method 2 with the variable velocity correction (b) and Method 2 without the variable velocity correction on pelleted CuBTC.(c)*

## 3.4 Scaling-up from the Bohart-Adams model

It will be shown here, for the adsorption shown in *Section 3.3.1* with activated carbon as adsorbent with an input concentration of $CO_2$ of 50%, the procedure to take it to an industrial scale. As mentioned above, the scaling criterion is to keep constant the linear velocity, the diameter-height relationship D/H, and the physical properties of the fluid, which correspond to the kinematic, geometric and dynamic similarity. With these similarities we can easily determine the Geometric parameters of the equipment. The end point of the scaling is a plant with a capacity of 750 $m^3$/h. It is worth clarifying that a theoretical study of the scaling of an adsorption column will be shown using a simple

model such as Bohart-Adams, to carry out the practical scaling up to this end point a scaling with at least one intermediate stage is necessary. But the procedure is the same that we will show from a laboratory scale to a large scale as that which would be carried out from a laboratory scale to a pilot plant and from a pilot plant to a large scale.

The stoichiometric time, $t_s$, and the Bohart-Adams constant, $K_{BA}$, were calculated and the results are shown in *Section 3.3.1*. With these parameters and the laboratory equipment parameters, the sorbate capacity per unit of volume of bed, $N_0$, and the sorbate capacity per unit of mass of bed, $q_0$, were calculated using *Equations 22 and 23*.

$$N_0 = \frac{F_0 . C_0 . t_s}{Z . A} \qquad \textit{(Eq.22).}$$

$$q_0 = \frac{N_0 . Z . A}{M} \qquad \textit{(Eq.23).}$$

With these two parameters, the geometric parameters of the column calculated with the aforementioned similarities and using *Equation 2* the mass of adsorbent necessary for the new adsorption column is calculated, obtaining a value of: $1.85x10^6$ kg. With E*quation 23* we can calculate the new stoichiometric time, the obtained value is: $2{,}47x10^4$ min (411.933 h). Having the operating and geometric parameters of the new column is easily obtained using *Equation 20*, the new breakthrough curve.

*Table 8* shows the results obtained in the scaling and in *Figure 14* the new breakthrough curve.

*Table8. Parameter comparison of laboratory scale and large scale.*

| Parameters | | Laboratory Scale | Industrial Scale |
|---|---|---|---|
| Geometrics | Internal Diameter (m) | $2{,}18x10^4$ | 11,38 |
| | Section ($m^2$) | $3{,}73x10^4$ | $1{,}017x10^2$ |
| | Height (m) | 0,13 | 67,86 |
| Opereating | Linear Flow Rate (m/min) | 0,013 | 0,013 |
| | Inlet Concentration ($mol/m^3$) | 18,619 | 18,619 |
| | Volumetric Flow ($m^3$/min) | $5{,}0x10^6$ | 1,32 |
| | Adsorbent Weight (kg) | 0,013 | $1{,}85x10^6$ |
| | Bed length (m) | 0,09 | 46,98 |
| | Stoichiometric time (min) | 45,91 | $2{,}47x10^4$ |
| B-A | $K_{BA}$ | 0,00933 | |
| | $N_0$ | $1{,}27x10^2$ | |
| | $q_0$ | 0,329 | |

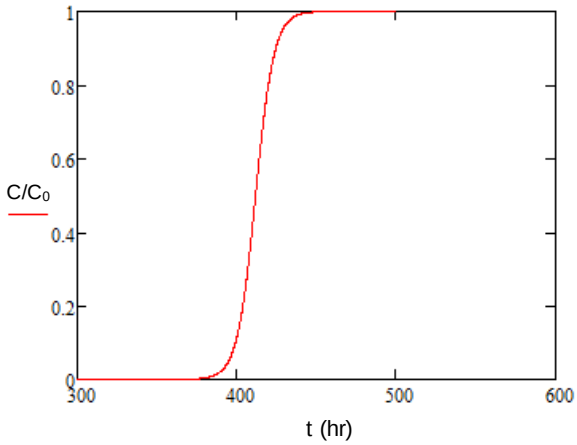


*Figure 14. Breakthrough curve for large scale with Activated carbon as adsorbent and $C_0$ =50% of $CO_2$.*

*Table 8* and *figure 14* show the result of the sizing of an adsorption column with a capacity of 750 $m^3$/h, these results were obtained in a simple way, with which the scaling process would be facilitated from the point of view of mathematical resolution.

# *Chapter 4* – CONCLUSIONS AND FUTURE PERSPECTIVES

## 4.1 Conclusions

In this work, alternatives were sought to transfer the mathematical simplicity of the Bohart-Adams model to gaseous processes where, due to the high concentration, the constant speed simplification of this model cannot be carried out. Also take advantage of that simple to carry out the scale-up of an adsorption process.

After analyzing the response of the Bohart-Adams equation in its different forms, with or without correction in stoichiometric time for velocity variation, with different adsorbents at different concentrations, it was observed that when using the sigmoid form of the equation of Bohart-Adams, with the correction of the stoichiometric time, a good fit is generally obtained for all concentrations with the three types of adsorbents used. In the particular case of activated carbon, the modeling is almost perfect for the three concentrations experienced. With the CuBTC adsorbent in its two forms (bulk and pelleted) for the highest initial concentration experienced (50% of $CO_2$), a slight difference was observed between the modeled curve and the experimental curve, although the improvement in the fit was also notable when the stoichiometric time was used with variable velocity correction.

The Bohart-Adams equation was designed with the work of analyzing the typical chlorine-charcoal transmission curve. The very good adjustment achieved using activated carbon as adsorbent in its three concentrations could be due to the physicochemical similarities with charcoal.

On the other hand, the differences between the modeled curve and the theoretical curve in the case of the pelleted and bulk CuBTC adsorbent with an initial concentration of 50%, may be due to the differences between the adsorptive capacity and the pore volume of the adsorbent as well as also the transfer mechanisms that the gas carries out according to the adsorbent with which it interacts, these differences that are not contemplated in the Bohart-Adamas equation. In these cases, the curve shows a delay in the theoretical curve. It was observed that using *method 2* with the correction for variable speed in stoichiometric time results in a good fit of the experimental data even with a 50% initial concentration of $CO_2$, with the activated carbon adsorbent. In the case of pelleted CuBTC and bulk CuBTC adsorbents, the adjustment is good up to 33% of

initial $CO_2$ concentration and with 50% a slight difference is observed with the experimental curve but a great improvement in the adjustment is also observed compared to adjustment without correction for speed variation in stoichiometric time.

In relation to the aforementioned, it was demonstrated that with the parameters calculated with the Bohart-Adams models, applying a series of simple steps we can scale the adsorption process, which is a powerful tool when designing and implementing a purification plant of biogas or any other where an adsorption process is involved, have a simple and not time consuming modeling and scaling method helps to economize this stage.

## 4.2 Future perspectives

A possible future perspective is to develop a model from the original differential equation of mass balance (Eq. 1) but considering the velocity variation variable. This leads to a system of coupled differential equations whose treatment increases significantly the mathematical complexity of the model and it will be interesting to compare the results with the ones obtained in this work. Steps in this direction have already been made and the work on a model based on the assumption of variable velocity has started to be carried out. Unfortunately, due to the restrictions and implications of current pandemic situation, a final result was not yet achieved.

# BIBLIOGRAPHIC REFERENCE


[1] Angelidaki, I., Treu, L., Tsapekos, P., Luo, G., Campanaro, S., Wenzel, H., & Kougias, P. G. (2018). Biogas upgrading and utilization: Current status and perspectives. *Biotechnology advances*, *36*(2), 452-466.

[2] Khan, I. U., Othman, M. H. D., Hashim, H., Matsuura, T., Ismail, A. F., Rezaei-DashtArzhandi, M., & Azelee, I. W. (2017). Biogas as a renewable energy fuel–A review of biogas upgrading, utilisation and storage. *Energy Conversion and Management*, *150*, 277-294.

[3] Peredo-Mancilla, D., Ghimbeu, C. M., Ho, B. N., Jeguirim, M., Hort, C., & Bessieres, D. (2019). Comparative study of the CH4/CO2 adsorption selectivity of activated carbons for biogas upgrading. *Journal of Environmental Chemical Engineering*, *7*(5), 103368.

[4] European Biogas Association, et al. Annual report 2018. 2019.

[5] Rasi, S., Veijanen, A., & Rintala, J. (2007). Trace compounds of biogas from different biogas production plants. *Energy*, *32*(8), 1375-1380.

[6] Jaffrin, A., Bentounes, N., Joan, A. M., & Makhlouf, S. (2003). Landfill biogas for heating greenhouses and providing carbon dioxide supplement for plant growth. *Biosystems engineering*, *86*(1), 113-123.

[7] Shin, H. C., Park, J. W., Park, K., & Song, H. C. (2002). Removal characteristics of trace compounds of landfill gas by activated carbon adsorption. *Environmental Pollution*, *119*(2), 227-236.

[8] Spiegel, R. J., & Preston, J. L. (2003). Technical assessment of fuel cell operation on anaerobic digester gas at the Yonkers, NY, wastewater treatment plant. *Waste management*, *23*(8), 709-717.

[9] Spiegel, R. J., & Preston, J. L. (2000). Test results for fuel cell operation on anaerobic digester gas. *Journal of Power Sources*, *86*(1-2), 283-288.

[10] Clark, S. (2008). Reform of the renewables obligation: statutory consultation on the Renewables Obligation Order 2009. UK Department of Business, Inovation & Skills (BIS), London, UK.

[11] Xu, Z., Cai, J. G., & Pan, B. C. (2013). Mathematically modeling fixed-bed adsorption in aqueous systems. *Journal of Zhejiang University SCIENCE A*, *14*(3), 155-176.

[12] Chu, K. H. (2010). Fixed bed sorption: setting the record straight on the Bohart–Adams and Thomas models. *Journal of Hazardous Materials*, *177*(1-3), 1006-1012.

[13] Ortiz, F. G., Aguilera, P. G., & Ollero, P. (2014). Modeling and simulation of the adsorption of biogas hydrogen sulfide on treated sewage–sludge. *Chemical Engineering Journal*, *253*, 305-315.

[14] Al Seadi, T. (2008). Biogas handbook.

[15] Hübner, T., & Mumme, J. (2015). Integration of pyrolysis and anaerobic digestion–use of aqueous liquor from digestate pyrolysis for biogas production. *Bioresource technology*, *183*, 86-92.

[16] Li, Y., Su, D., Luo, S., Jiang, H., Qian, M., Zhou, H., ... & Xu, Q. (2017). Pyrolysis gas as a carbon source for biogas production via anaerobic digestion. *RSC advances*, *7*(66), 41889-41895.

[17] Ryckebosch, E., Drouillon, M., & Vervaeren, H. (2011). Techniques for transformation of biogas to biomethane. *Biomass and bioenergy*, *35*(5), 1633-1645.

[18] Pertl, A., Mostbauer, P., & Obersteiner, G. (2010). Climate balance of biogas upgrading systems. *Waste management*, *30*(1), 92-99.

[19] Sun, Q., Li, H., Yan, J., Liu, L., Yu, Z., & Yu, X. (2015). Selection of appropriate biogas upgrading technology-a review of biogas cleaning, upgrading and utilisation. *Renewable and Sustainable Energy Reviews*, *51*, 521-532.

[20] Chen, X. Y., Vinh-Thang, H., Ramirez, A. A., Rodrigue, D., & Kaliaguine, S. (2015). Membrane gas separation technologies for biogas upgrading. *Rsc Advances*, *5*(31), 24399-24448.

[21] Hahn, H., Hartmann, K., Bühle, L., & Wachendorf, M. (2015). Comparative life cycle assessment of biogas plant configurations for a demand oriented biogas supply for flexible power generation. *Bioresource technology*, *179*, 348-358.

[22] Svensson, M. (2014). Biomethane standards: Gas quality standardisation of biomethane, going from national to international level. In *European workshop Biomethane, Brussels. Green Gas Grids*.

[23] Ho, M. T., Allinson, G. W., & Wiley, D. E. (2008). Reducing the cost of CO2 capture from flue gases using pressure swing adsorption. *Industrial & Engineering Chemistry Research*, *47*(14), 4883-4890.

[24] Cavenati, S., Grande, C. A., & Rodrigues, A. E. (2005). Upgrade of methane from landfill gas by pressure swing adsorption. *Energy & fuels*, *19*(6), 2545-2555.

[25] Reijenga, J. C., Bini, L., Maassen, J. I., Van Meel, P. A., De Hullu, J., Shazad, S., & Vaessen, J. M. (2008). Comparing different biogas upgrading techniques. *Interim Report, Eindhoven University of Technology*.

[26] Plaza, M. G., García, S., Rubiera, F., Pis, J. J., & Pevida, C. (2010). Post-combustion CO2 capture with a commercial activated carbon: comparison of different regeneration strategies. *Chemical Engineering Journal*, *163*(1-2), 41-47.

[27] Mason, J. A., Sumida, K., Herm, Z. R., Krishna, R., & Long, J. R. (2011). Evaluating metal–organic frameworks for post-combustion carbon dioxide capture via temperature swing adsorption. *Energy & Environmental Science*, *4*(8), 3030-3040.

[28] Moon, S. H., & Shim, J. W. (2006). A novel process for CO2/CH4 gas separation on activated carbon fibers—electric swing adsorption. *Journal of colloid and interface science*, *298*(2), 523-528.

[29] Cozma, P., Wukovits, W., Mămăligă, I., Friedl, A., & Gavrilescu, M. (2015). Modeling and simulation of high pressure water scrubbing technology applied for biogas upgrading. *Clean Technologies and Environmental Policy*, *17*(2), 373-391.

[30] Petersson, A., & Wellinger, A. (2009). Biogas upgrading technologies–developments and innovations. *IEA bioenergy*, *20*, 1-19.

[31] Tippayawong, N., & Thanompongchart, P. (2010). Biogas quality upgrade by simultaneous removal of CO2 and H2S in a packed column reactor. *Energy*, *35*(12), 4531-4535.

[32] Zhao, Q., Leonhardt, E., MacConnell, C., Frear, C., & Chen, S. (2010). Purification technologies for biogas generated by anaerobic digestion. *Compressed Biomethane, CSANR, Ed*, *24*.

[33] Kismurtono, M. (2011). Upgrade biogas purification in packed column with chemical absorption of CO2 for energy alternative of small industry (UKM-Tahu). *Int J Eng Technol*, *11*(1), 59-62.

[34] Privalova, E., Rasi, S., Mäki-Arvela, P., Eränen, K., Rintala, J., Murzin, D. Y., & Mikkola, J. P. (2013). CO 2 capture from biogas: absorbent selection. *RSC advances*, *3*(9), 2979-2994.

[35] Huang, H., Chang, S. G., & Dorchak, T. (2002). Method to regenerate ammonia for the capture of carbon dioxide. *Energy & fuels*, *16*(4), 904-910.

[36] Jiang, L. Y., Chung, T. S., & Kulprathipanja, S. (2006). An investigation to revitalize the separation performance of hollow fibers with a thin mixed matrix composite skin for gas separation. *Journal of membrane science*, *276*(1-2), 113-125.

[37] Rongwong, W., Boributh, S., Assabumrungrat, S., Laosiripojana, N., & Jiraratananon, R. (2012). Simultaneous absorption of CO2 and H2S from biogas by capillary membrane contactor. *Journal of membrane science*, *392*, 38-47.

[38] Baker, R. W., & Lokhandwala, K. (2008). Natural gas processing with membranes: an overview. *Industrial & Engineering Chemistry Research*, *47*(7), 2109-2121.

[39] Basu, S., Khan, A. L., Cano-Odena, A., Liu, C., & Vankelecom, I. F. (2010). Membrane-based technologies for biogas separations. *Chemical Society Reviews*, *39*(2), 750-768.

[40] Robeson, L. M. (2008). The upper bound revisited. *Journal of membrane science*, *320*(1-2), 390-400.

[41] Barboiu, C., Sala, B., Bec, S., Pavan, S., Petit, E., Colomban, P., ... & Hittner, D. (2009). Structural and mechanical characterizations of microporous silica–boron membranes for gas separation. *Journal of Membrane Science*, *326*(2), 514-525.

[42] Rezaei, M., Ismail, A. F., Hashemifard, S. A., & Matsuura, T. (2014). Preparation and characterization of PVDF-montmorillonite mixed matrix hollow fiber membrane for gas–liquid contacting process. *Chemical Engineering Research and Design*, *92*(11), 2449-2460.

[43] Rezaei-DashtArzhandi, M., Ismail, A. F., Ghanbari, M., Bakeri, G., Hashemifard, S. A., Matsuura, T., & Moslehyani, A. (2016). An investigation of temperature effects on the properties and CO2 absorption performance of porous PVDF/montmorillonite mixed matrix membranes. *Journal of Natural Gas Science and Engineering*, *31*, 515-524.

[44] Aroon, M. A., Ismail, A. F., Matsuura, T., & Montazer-Rahmati, M. M. (2010). Performance studies of mixed matrix membranes for gas separation: a review. *Separation and purification Technology*, *75*(3), 229-242.

[45] Andriani, D., Wresta, A., Atmaja, T. D., & Saepudin, A. (2014). A review on optimization production and upgrading biogas through $CO_2$ removal using various techniques. *Applied biochemistry and biotechnology*, *172*(4), 1909-1928.

[46] Zanganeh, K. E., Shafeen, A., & Salvador, C. (2009). CO2 capture and development of an advanced pilot-scale cryogenic separation and compression unit. *Energy Procedia*, *1*(1), 247-252.

[47] Krich, K., Augenstein, A., Batmale, J., Benemann, J., Rutledge, B., & Salour, D. (2005). Upgrading dairy biogas to biomethane and other fuels. *Biomethane from dairy waste-A sourcebook for the production and use of renewable natural gas in California. California: Clear Concepts*, 47-69.

[48] Jürgensen, L., Ehimen, E. A., Born, J., & Holm-Nielsen, J. B. (2014). Utilization of surplus electricity from wind power for dynamic biogas upgrading: Northern Germany case study. *biomass and bioenergy*, *66*, 126-132.

[49] Agler, M. T., Wrenn, B. A., Zinder, S. H., & Angenent, L. T. (2011). Waste to bioproduct conversion with undefined mixed cultures: the carboxylate platform. *Trends in biotechnology*, *29*(2), 70-78.

[50] Kennes, D., Abubackar, H. N., Diaz, M., Veiga, M. C., & Kennes, C. (2016). Bioethanol production from biomass: carbohydrate vs syngas fermentation. *Journal of Chemical Technology & Biotechnology*, *91*(2), 304-317.

[51] Lu, L., & Ren, Z. J. (2016). Microbial electrolysis cells for waste biorefinery: A state of the art review. *Bioresource technology*, *215*, 254-264.

[52] Zhang, Y., & Angelidaki, I. (2014). Microbial electrolysis cells turning to be versatile technology: recent advances and future challenges. *Water research*, *56*, 11-25.

[53] Cheng, S., Xing, D., Call, D. F., & Logan, B. E. (2009). Direct biological conversion of electrical current into methane by electromethanogenesis. *Environmental science & technology*, *43*(10), 3953-3958.

[54] Villano, M., Aulenta, F., Ciucci, C., Ferri, T., Giuliano, A., & Majone, M. (2010). Bioelectrochemical reduction of CO2 to CH4 via direct and indirect extracellular electron transfer by a hydrogenophilic methanogenic culture. *Bioresource technology*, *101*(9), 3085-3090.

[55] Kougias, P. G., Boe, K., Einarsdottir, E. S., & Angelidaki, I. (2015). Counteracting foaming caused by lipids or proteins in biogas reactors using rapeseed oil or oleic acid as antifoaming agents. *Water Research*, *79*, 119-127.

[56] Kougias, P. G., Treu, L., Campanaro, S., Zhu, X., & Angelidaki, I. (2016). Dynamic functional characterization and phylogenetic changes due to Long Chain Fatty Acids pulses in biogas reactors. *Scientific reports*, *6*, 28810.

[57] Bauer, F., Persson, T., Hulteberg, C., & Tamm, D. (2013). Biogas upgrading–technology overview, comparison and perspectives for the future. *Biofuels, Bioproducts and Biorefining*, *7*(5), 499-511.

[58] Weiland, P. (2010). Biogas production: current state and perspectives. *Applied microbiology and biotechnology*, *85*(4), 849-860.

[59] Abatzoglou, N., & Boivin, S. (2009). A review of biogas purification processes. *Biofuels, Bioproducts and Biorefining*, *3*(1), 42-71.

[60] Kárászová, M., Sedláková, Z., & Izák, P. (2015). Gas permeation processes in biogas upgrading: A short review. *Chemical Papers*, *69*(10), 1277-1283.

[61] Bekkering, J., Broekhuis, A. A., & Van Gemert, W. J. T. (2010). Optimisation of a green gas supply chain–A review. *Bioresource technology*, *101*(2), 450-456.

[62] Chandra, R., Vijay, V. K., & Subbarao, P. M. V. (2012). Vehicular quality biomethane production from biogas by using an automated water scrubbing system. *ISRN Renewable Energy*, *2012*.

[63] Bauer, F., Hulteberg, C., Persson, T., & Tamm, D. (2013). *Biogas upgrading-Review of commercial technologies*. Svenskt gastekniskt center.

[64] Stern, S. A., Krishnakumar, B., Charati, S. G., Amato, W. S., Friedman, A. A., & Fuess, D. J. (1998). Performance of a bench-scale membrane pilot plant for the upgrading of biogas in a wastewater treatment plant. *Journal of membrane science*, *151*(1), 63-74.

[65] Olajire, A. A. (2010). CO2 capture and separation technologies for end-of-pipe applications–a review. *Energy*, *35*(6), 2610-2628.

[66] Molino, A., Migliori, M., Ding, Y., Bikson, B., Giordano, G., & Braccio, G. (2013). Biogas upgrading via membrane process: modelling of pilot plant scale and the end uses for the grid injection. *Fuel*, *107*, 585-592.

[67] Baker, R. W. (2002). Future directions of membrane gas separation technology. *Industrial & engineering chemistry research*, *41*(6), 1393-1411.

[68] Xu, Y., Huang, Y., Wu, B., Zhang, X., & Zhang, S. (2015). Biogas upgrading technologies: Energetic analysis and environmental impact assessment. *Chinese Journal of Chemical Engineering*, *23*(1), 247-254.

[69] De Hullu, J., Maassen, J. I. W., Van Meel, P. A., Shazad, S., Vaessen, J. M. P., Bini, L., & Reijenga, J. C. (2008). Comparing different biogas upgrading techniques. *Eindhoven University of Technology, The Netherlands*.

[70] Molino, A., Nanna, F., Ding, Y., Bikson, B., & Braccio, G. (2013). Biomethane production by anaerobic digestion of organic waste. *Fuel*, *103*, 1003-1009.

[71] Axelsson, L., Franzén, M., Ostwald, M., Berndes, G., Lakshmi, G., & Ravindranath, N. H. (2012). Jatropha cultivation in southern India: assessing farmers' experiences. *Biofuels, Bioproducts and Biorefining*, *6*(3), 246-256.

[72] Augelletti, R., Conti, M., & Annesini, M. C. (2017). Pressure swing adsorption for biogas upgrading. A new process configuration for the separation of biomethane and carbon dioxide. *Journal of Cleaner Production*, *140*, 1390-1398.

[73] Awe, O. W., Zhao, Y., Nzihou, A., Minh, D. P., & Lyczko, N. (2017). A review of biogas utilisation, purification and upgrading technologies. *Waste and Biomass Valorization*, *8*(2), 267-283.

[74] Abd, A. A., Naji, S. Z., Hashim, A. S., & Othman, M. R. (2020). Carbon dioxide removal through Physical Adsorption using Carbonaceous and non-Carbonaceous Adsorbents: A review. *Journal of Environmental Chemical Engineering*, 104142.

[75] Grande, C. A., & Rodrigues, A. E. (2007). Biogas to fuel by vacuum pressure swing adsorption I. Behavior of equilibrium and kinetic-based adsorbents. *Industrial & engineering chemistry research*, *46*(13), 4595-4605.

[76] Li, J. R., Ma, Y., McCarthy, M. C., Sculley, J., Yu, J., Jeong, H. K., ... & Zhou, H. C. (2011). Carbon dioxide capture-related gas adsorption and separation in metal-organic frameworks. *Coordination Chemistry Reviews*, *255*(15-16), 1791-1823.

[77] Bui, M., Adjiman, C. S., Bardow, A., Anthony, E. J., Boston, A., Brown, S., ... & Hallett, J. P. (2018). Carbon capture and storage (CCS): the way forward. *Energy & Environmental Science*, *11*(5), 1062-1176.

[78] Gray, M. L., Champagne, K. J., Fauth, D., Baltrus, J. P., & Pennline, H. (2008). Performance of immobilized tertiary amine solid sorbents for the capture of carbon dioxide. *International Journal of Greenhouse Gas Control*, *2*(1), 3-8.

[79] Samanta, A., Zhao, A., Shimizu, G. K., Sarkar, P., & Gupta, R. (2012). Post-combustion CO2 capture using solid sorbents: a review. *Industrial & Engineering Chemistry Research*, *51*(4), 1438-1463.

[80] Lozano-Castelló, D., Cazorla-Amorós, D., Linares-Solano, A., & Quinn, D. F. (2002). Activated carbon monoliths for methane storage: influence of binder. *Carbon*, *40*(15), 2817-2825.

[81] Bilalis, P., Katsigiannopoulos, D., Avgeropoulos, A., & Sakellariou, G. (2014). Non-covalent functionalization of carbon nanotubes with polymers. *Rsc Advances*, *4*(6), 2911-2934.

[82] Yaumi, A. L., Bakar, M. A., & Hameed, B. H. (2017). Recent advances in functionalized composite solid materials for carbon dioxide capture. *Energy*, *124*, 461-480.

[83] Tong, L., Yue, T., Zuo, P., Zhang, X., Wang, C., Gao, J., & Wang, K. (2017). Effect of characteristics of KI-impregnated activated carbon and flue gas components on Hg0 removal. *Fuel*, *197*, 1-7.

[84] Wang, J., Huang, L., Yang, R., Zhang, Z., Wu, J., Gao, Y., ... & Zhong, Z. (2014). Recent advances in solid sorbents for CO 2 capture and new development trends. *Energy & Environmental Science*, *7*(11), 3478-3518.

[85] Silvestre-Albero, J., Wahby, A., Sepúlveda-Escribano, A., Martínez-Escandell, M., Kaneko, K., & Rodríguez-Reinoso, F. (2011). Ultrahigh $CO_2$ adsorption capacity on carbon molecular sieves at room temperature. *Chemical Communications*, *47*(24), 6840-6842.

[86] Zhang, X., Lu, W., Zhou, G., & Li, Q. (2020). Understanding the mechanical and conductive properties of carbon nanotube fibers for smart electronics. *Advanced Materials*, *32*(5), 1902028.

[87] Mirka, B., Fong, D., Rice, N. A., Melville, O. A., Adronov, A., & Lessard, B. H. (2019). Polyfluorene-Sorted Semiconducting Single-Walled Carbon Nanotubes for Applications in Thin-Film Transistors. *Chemistry of Materials*, *31*(8), 2863-2872.

[88] Gupta, N., Gupta, S. M., & Sharma, S. K. (2019). Carbon nanotubes: synthesis, properties and engineering applications. *Carbon Letters*, 1-29.

[89] Dai, H., Wong, E. W., & Lieber, C. M. (1996). Probing electrical transport in nanomaterials: conductivity of individual carbon nanotubes. *Science*, *272*(5261), 523-526.

[90] Berber, S., Kwon, Y. K., & Tománek, D. (2000). Unusually high thermal conductivity of carbon nanotubes. *Physical review letters*, *84*(20), 4613.

[91] Kim, P., Shi, L., Majumdar, A., & McEuen, P. L. (2001). Thermal transport measurements of individual multiwalled nanotubes. *Physical review letters*, *87*(21), 215502.

[92] Behera, R. P., Rawat, P., Tiwari, S. K., & Singh, K. K. (2020). A brief review on the mechanical properties of Carbon nanotube reinforced polymer composites. *Materials Today: Proceedings*, *22*, 2109-2117.

[93] Thangavel, S., & Venugopal, G. (2014). Understanding the adsorption property of graphene-oxide with different degrees of oxidation levels. *Powder technology*, *257*, 141-148.

[94] Fakhri, A. (2017). Adsorption characteristics of graphene oxide as a solid adsorbent for aniline removal from aqueous solutions: Kinetics, thermodynamics and mechanism studies. *Journal of Saudi Chemical Society*, *21*, S52-S57.

[95] Baig, N., Sajid, M., & Saleh, T. A. (2019). Graphene-based adsorbents for the removal of toxic organic pollutants: a review. *Journal of environmental management*, *244*, 370-382.

[96] Khan, N. A., Hasan, Z., & Jhung, S. H. (2013). Adsorptive removal of hazardous materials using metal-organic frameworks (MOFs): a review. *Journal of hazardous materials*, *244*, 444-456.

[97] Alhamami, M., Doan, H., & Cheng, C. H. (2014). A review on breathing behaviors of metal-organic-frameworks (MOFs) for gas adsorption. *Materials*, *7*(4), 3198-3250.

[98] Chester, A. W., & Derouane, E. G. (2009). *Zeolite characterization and catalysis* (Vol. 360). New York: Springer.

[99] Zhang, J., Singh, R., & Webley, P. A. (2008). Alkali and alkaline-earth cation exchanged chabazite zeolites for adsorption based CO2 capture. *Microporous and Mesoporous Materials*, *111*(1-3), 478-487.

[100] Harlick, P. J., & Sayari, A. (2006). Applications of pore-expanded mesoporous silicas. 3. Triamine silane grafting for enhanced $CO_2$ adsorption. *Industrial & Engineering Chemistry Research*, *45*(9), 3248-3255.

[101] Qin, C., Yin, J., Ran, J., Zhang, L., & Feng, B. (2014). Effect of support material on the performance of K2CO3-based pellets for cyclic $CO_2$ capture. *Applied energy*, *136*, 280-288.

[102] Sanz-Pérez, E. S., Arencibia, A., Calleja, G., & Sanz, R. (2018). Tuning the textural properties of HMS mesoporous silica. Functionalization towards $CO_2$ adsorption. *Microporous and Mesoporous Materials*, *260*, 235-244.

[103] Hori, K., Higuchi, T., Aoki, Y., Miyamoto, M., Oumi, Y., Yogo, K., & Uemiya, S. (2017). Effect of pore size, aminosilane density and aminosilane molecular length on $CO_2$ adsorption performance in aminosilane modified mesoporous silica. *Microporous and Mesoporous Materials*, *246*, 158-165.

[104] Hakiki, A., Boukoussa, B., Zahmani, H. H., Hamacha, R., Abdelkader, N. E. H. H., Bekkar, F., ... & Azzouz, A. (2018). Synthesis and characterization of mesoporous silica SBA-15 functionalized by mono-, di-, and tri-amine and its catalytic behavior towards Michael addition. *Materials Chemistry and Physics*, *212*, 415-425.

[105] Lee, S. Y., & Park, S. J. (2015). A review on solid adsorbents for carbon dioxide capture. *Journal of Industrial and Engineering Chemistry*, *23*, 1-11.

[106] Rangnekar, N., Mittal, N., Elyassi, B., Caro, J., & Tsapatsis, M. (2015). Zeolite membranes–a review and comparison with MOFs. *Chemical Society Reviews*, *44*(20), 7128-7154.

[107] Chu, K. H. (2020). Breakthrough curve analysis by simplistic models of fixed bed adsorption: In defense of the century-old Bohart-Adams model. *Chemical Engineering Journal*, *380*, 122513.

[108] Dennis Jr, J. E., Gay, D. M., & Welsch, R. E. (1981). Algorithm 573: NL2SOL—an adaptive nonlinear least-squares algorithm [E4]. *ACM Transactions on Mathematical Software (TOMS)*, *7*(3), 369-383.

[109] Ruthven, D. M. (1984). *Principles of adsorption and adsorption processes*. John Wiley & Sons.

[110] Bohart, G. S., & Adams, E. Q. (1920). Some aspects of the behavior of charcoal with respect to chlorine. *Journal of the American Chemical Society*, *42*(3), 523-544.

[111] Cooney, D. O. (1999). Adsorption design for wastewater treatment, CRC Pres. *INC., Boca Raton, Florida, USA*.

[112] Amundson, N. R. (1948). A Note on the Mathematics of Adsorption in Beds. *The Journal of Physical Chemistry*, *52*(7), 1153-1157.

[113] Guibal, E., Lorenzelli, R., Vincent, T., & Cloirec, P. L. (1995). Application of silica gel to metal ion sorption: static and dynamic removal of uranyl ions. *Environmental technology*, *16*(2), 101-114.

[114] Al-Janabi, N., Vakili, R., Kalumpasut, P., Gorgojo, P., Siperstein, F. R., Fan, X., & McCloskey, P. (2018). Velocity variation effect in fixed bed columns: A case study of $CO_2$ capture using porous solid adsorbents. *AIChE Journal*, *64*(6),

2189-2197.

[115] Malek, A., Farooq, S., Rathor, M. N., & Hidajat, K. (1995). Effect of velocity variation due to adsorption-desorption on equilibrium data from breakthrough experiments. *Chemical engineering science*, *50*(4), 737-740.

[116] Khan, M. M. U. R., Hossain, M. R., & Parvin, S. (2017). Numerical integration schemes for unequal data spacing. *American Journal of Applied Mathematics*, *5*(2), 48-56.